Ets2 Determines the Inflammatory State of Endothelial Cells in Advanced Atherosclerotic Lesions

Caroline Cheng, Dennie Tempel, Wijnand K. Den Dekker, Remco Haasdijk, Ihsan Chrifi, Frank L. Bos, Kim Wagtmans, Esther H. van de Kamp, Lau Blonden, Erik A.L. Biessen, Frans Moll, Gerard Pasterkamp, Patrick W. Serruys, Stefan Schulte-Merker and Henricus J. Duckers

Circulation Research 2011, 109:382-395: originally published online June 23, 2011
doi: 10.1161/CIRCRESAHA.111.243444
Circulation Research is published by the American Heart Association. 7272 Greenville Avenue, Dallas, TX 72514
 Print ISSN: 0009-7330. Online ISSN: 1524-4571

Ets2 Determines the Inflammatory State of Endothelial Cells in Advanced Atherosclerotic Lesions

Caroline Cheng, Dennie Tempel, Wijnand K. Den Dekker, Remco Haasdijk, Ihsan Chrifi, Frank L. Bos, Kim Wagtmans, Esther H. van de Kamp, Lau Blonden, Erik A.L. Biessen, Frans Moll, Gerard Pasterkamp, Patrick W. Serruys, Stefan Schulte-Merker, Henricus J. Duckers

Rationale: **Neovascularization is required for embryonic development and plays a central role in diseases in adults. In atherosclerosis, the role of neovascularization remains to be elucidated. In a genome-wide microarray-screen of Flk1+ angioblasts during murine embryogenesis, the v-ets erythroblastosis virus E26 oncogene homolog 2 (Ets2) transcription factor was identified as a potential angiogenic factor.**

Objectives: **We assessed the role of Ets2 in endothelial cells during atherosclerotic lesion progression toward plaque instability.**

Methods and Results: **In 91 patients treated for carotid artery disease, Ets2 levels showed modest correlations with capillary growth, thrombogenicity, and rising levels of tumor necrosis factor-α (TNFα), monocyte chemoattractant protein 1, and interleukin-6 in the atherosclerotic lesions. Experiments in ApoE$^{-/-}$ mice, using a vulnerable plaque model, showed that Ets2 expression was increased under atherogenic conditions and was augmented specifically in the vulnerable versus stable lesions. In endothelial cell cultures, Ets2 expression and activation was responsive to the atherogenic cytokine TNFα. In the murine vulnerable plaque model, overexpression of Ets2 promoted lesion growth with neovessel formation, hemorrhaging, and plaque destabilization. In contrast, Ets2 silencing, using a lentiviral shRNA construct, promoted lesion stabilization. In vitro studies showed that Ets2 was crucial for TNFα-induced expression of monocyte chemoattractant protein 1, interleukin-6, and vascular cell adhesion molecule 1 in endothelial cells. In addition, Ets2 promoted tube formation and amplified TNFα-induced loss of vascular endothelial integrity. Evaluation in a murine retina model further validated the role of Ets2 in regulating vessel inflammation and endothelial leakage.**

Conclusions: **We provide the first evidence for the plaque-destabilizing role of Ets2 in atherosclerosis development by induction of an intraplaque proinflammatory phenotype in endothelial cells. (*Circ Res*. 2011;109:382-395.)**

Key Words: angiogenesis ■ atherosclerosis ■ endothelium ■ vascular inflammation ■ vulnerable plaque

Atherosclerosis is a complex disease with a strong inflammatory component,[1–4] initially triggered by endothelial dysfunction and characterized by an influx of atherogenic lipoprotein components, combined with endothelial upregulation of proinflammatory cytokines and adhesion molecules.[5] Monocyte adhesion and extravasation perpetuate the disease by further differentiation into macrophages and foam cells, ultimately driving atherosclerotic lesion growth and complexity.[6] Vulnerable plaque (VP) is an advanced form of atherosclerosis, characterized by an exuberated inflammatory response with the formation of a large necrotic core, and a rupture-prone thin fibrous cap.[7] In these VPs, microvessel formation with extravasation of erythrocytes in the vasa vasorum and intimal area has been observed.[8–10] Although new vessel formation in advanced atherosclerosis has been associated with lesion progression and instability,[10–12] the exact molecular mechanisms that facilitate neovascularization in atherosclerosis must be further elucidated.

Recently, we have conducted a genome-wide screen to identify new genetic regulators of angiogenesis. The v-ets erythroblastosis virus E26 oncogene homolog 2 (Ets2) transcription factor was shown to be upregulated during murine embryonic angiogenesis in Flk1+ angioblasts. Expression of Ets2 in the vascular bed was also verified in developing zebra fish by whole mount in situ hybridization. Ets2 belongs to a family of transcription factors that share the E26 Transformation-specific Sequence (Ets) domain that recognizes a specific core sequence (5′-GGAA/T-3′). This functional domain is conserved in differ-

Original received March 7, 2011; revision received June 15, 2011; accepted June 15, 2011. In May 2011, the average time from submission to first decision for all original research papers submitted to *Circulation Research* was 14.5 days.

From the Molecular Cardiology Laboratory, Experimental Cardiology, Thoraxcenter, Erasmus University Medical Center, Rotterdam, The Netherlands (C.C., D.T., W.K.D.D., R.H., I.C., F.L.B., K.W., E.v.d.K., L.B., P.W.S., H.J.D.); Hubrecht's Institute-KNAW and University Medical Centre, Utrecht, The Netherlands (F.L.B., S.S.-M.); the Department of Pathology, Maastricht University Medical Center, Maastricht, The Netherlands (E.A.L.B.); and the Departments of Vascular Surgery (F.M.) and Cardiology (G.P.), University Medical Center Utrecht, Utrecht, The Netherlands.

Correspondence to H.J. Duckers, MD, PhD, FESC, Molecular Cardiology Laboratory, Room Ee2389a, Thoraxcenter, Erasmus University Medical Center, s'Gravendijksewal 230 3015 GE Rotterdam, The Netherlands. E-mail h.duckers@erasmusmc.nl

Circulation Research **is available at http://circres.ahajournals.org** **DOI: 10.1161/CIRCRESAHA.111.243444**

ent species.[13] Ets2 has been shown to be a potent transactivator of angiogenic regulators, including vascular endothelial cell growth factor receptor (VEGFR)1,[14] heme oxygenase 1 (HO-1),[15] and cluster of differentiation 13 (CD13)/APN.[16] Ets2 was also studied in immune activation and was shown to be involved in the transcriptional regulation of cytokines including interleukin (IL)5[17] and IL12p40,[18] suggesting a prominent role in immune response regulation.

We postulated that Ets2 could mediate immune-activation of the endothelium in the late phase of atherosclerosis development, as well as promoting monocyte adhesion via neovessel activation. In addition, Ets2 might be an important modulator in microvessel formation of the vasa vasorum in atherosclerotic lesions and thus contribute to plaque destabilization in advanced lesions. We show that Ets2 induces atherosclerotic plaque destabilization by promoting an endothelial cell (EC) phenotype of enhanced inflammatory state.

Non-standard Abbreviations and Acronyms

ADAM10	A disintegrin and metalloprotease 10
Ang	angiopoietin
Apo	apolipoprotein
CEA	carotid endarterectomy
CD13	cluster of differentiation 13
CD45	cluster of differentiation 45
CD68	cluster of differentiation 68
DLL4	delta-like 4 ligand
ECs	endothelial cells
EphB4	ephrin receptor B4
Ets	v-ets erythroblastosis virus E26 oncogene homolog
Flk1	fetal liver kinase 1
HO-1	heme oxygenase 1
IL	interleukin
IPH	intraplaque hemorrhaging
LDL	low-density lipoprotein
MCP1	monocyte chemoattractant protein 1
MMP	matrix metalloproteinase
oxLDL	oxidized low-density lipoprotein
shRNA	Short hairpin RNA
TNFα	tumor necrosis factor-α
VCAM1	vascular cell adhesion molecule 1
VEGFA	vascular endothelial cell growth factor A
VEGFR1	vascular endothelial cell growth factor receptor 1
VEGFR2	vascular endothelial cell growth factor receptor 2
Ve-cadherin	vascular endothelial-cadherin
qPCR	quantitative polymerase chain reaction
VP	vulnerable plaque

Methods

Analysis of Human Atherosclerotic Plaques in Human Carotid Endarterectomy Specimens

Atherosclerosis samples were obtained from a biobank collection of endarterectomy-derived specimens of patients who had been diagnosed with symptomatic carotid artery disease (Athero Express Biobank, University Medical Center Utrecht, The Netherlands). The study was approved by an institutional review committee, and all the subjects involved provided informed consent. Samples had been processed for immunohistological analysis, as well as protein extraction, and were quantified by 2 independent observers for histomorphological indices of plaque vulnerability, as reported earlier.[19]

Vulnerable Plaque Model in Apolipoprotein $E^{-/-}$ Mice

All experiments were conducted in compliance with institutional (Erasmus University Medical Center, Rotterdam, The Netherlands) and national guidelines. apolipoprotein (Apo)$E^{-/-}$ mice (12 to 25 weeks; Jackson Laboratory, Bar Harbor, ME) on a Western-type diet (diet W, Hope Farms, The Netherlands) were anesthetized by isoflurane inhalation and received a cast implantation in the right common carotid artery position. At 6 weeks after cast placement, animals were anesthetized, and 50 μL of 1×10^{10} pfu/mL recombinant adenovirus (either Ets2-Ad or ΔE1-Ad, v/v 1:1) or lentivirus (either LV-siEts2 or LV-sisham, vol/vol 1:1) mixed with pluronic gel (Sigma, The Netherlands) was applied to the adventitia proximal to the cast, the predicted location of the vulnerable plaque. After an incubation time of 10 minutes, the gel was coagulated and the wound was closed; 21 days later, the carotid arteries were harvested for histological and immunohistochemical analysis.

Retina Transfection in $ApoE^{-/-}$ Mice

$ApoE^{-/-}$ mice (12 to 15 weeks; Jackson Laboratory, Bar Harbor, ME) were anesthetized by isoflurane inhalation and received intravitreal microinjection of 2 μL of 0.5×10^{10} pfu/mL recombinant adenovirus (either Ets2-Ad or ΔE1-Ad). Animals were allowed to recover and were euthanized 2 days after injections.

Tube Formation Assays

In vitro formation of tube structures was studied on BioCoat Matrigel tissue culture plates (BD Biosciences, Alphen a/d Rijn, The Netherlands). SiRNA-transfected HUVECs were plated at 30 000 cells/well in 96-well plates precoated with a solution of Matrigel basement membrane matrix. After 24 hours of incubation at 37°C, cells were visualized by Calcein-Am uptake (BD Biosciences). Tube organization was examined using an inverted fluorescence microscopy, and the photographs were subsequently analyzed using the commercial image analysis system (AngioSys, Buckingham, UK). Statistical analysis was performed using 1-way ANOVA. Data are presented as mean±SEM; probability values <0.05 were considered significant.

Full protocol descriptions of the material and methods are provided in the Online supplemental data available online at http://circres.ahajournals.org.

Results

Ets2 Levels Correlate With Intraplaque Microvessel Formation and Levels of Proinflammatory Cytokines in Human Vulnerable Atherosclerotic Plaques

Ets2 protein levels were quantified by ELISA in carotid endarterectomy (CEA) specimens obtained from patients with documented symptomatic carotid artery disease. A full-length recombinant Ets2 protein was used as a positive control and for assay calibration. Patients were categorized into quartiles according to Ets2 levels (Online Table I, supplemental data). No significant differences were observed in patient characteristics and cardiovascular risk factors between quartiles. Online Table II in the supplemental data depicts baseline characteristics of the patient group. The mean Ets2 level in the CEA samples was 373.2±34.4 ng/mL.

Rising Ets2 levels correlated with increased intraplaque capillary density in the CEA specimen ($R=0.27$; $P=0,01$;

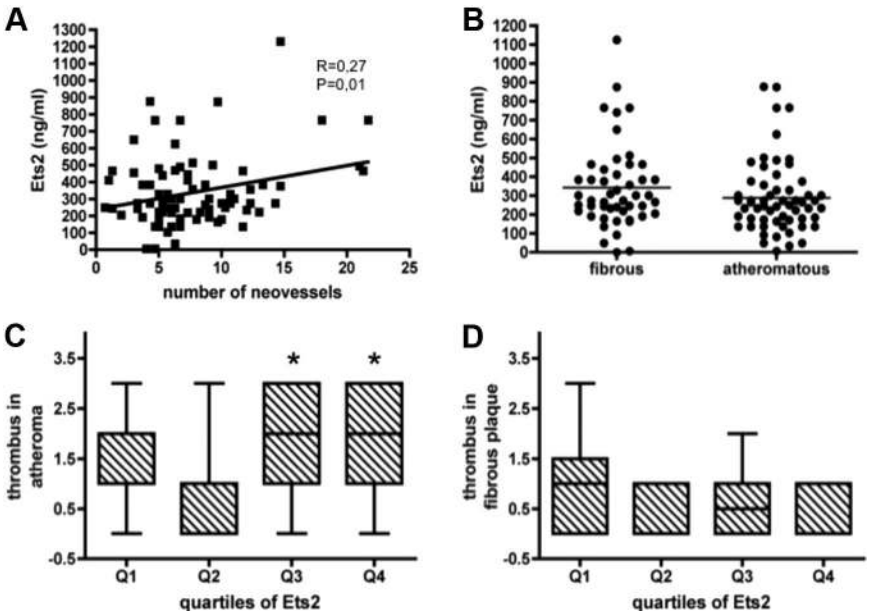

Figure 1. Ets2 expression in human atherosclerotic lesions correlates with intraplaque neovascularization and increased thrombogenicity in human atheroma. A, Ets2 levels correlated with intraplaque neovascularization ($R=0.27$; $P=0.01$) but was not upregulated in human atheromatous atherosclerotic lesions compared with fibrous plaques (**B**) ($P=0.12$). **C**, Ets2 levels correlated with thrombogenicity in human atheromas (*$P<0.05$; versus Q2) but not in fibrous plaques (**D**). Values of plaque thrombogenicity were divided into 4 quartiles ranging form 0 (representing the group of patients with the lowest percentage) to 3 (representing the group of patients with the highest percentage) on the *Y*-axes. On the *X*-axes, Ets2 protein levels are shown, divided into 4 quartiles ranging from Q1 (representing the group of patients with the lowest percentage) to Q4 (representing the group of patients with the highest percentage).

Figure 1A), but mean Ets2 levels do not differ between stable fibrous or vulnerable atheromatous plaque phenotype ($P=0.18$; Figure 1B). Ets2 protein levels specifically correlated with increased plaque thrombogenicity and erythrocyte extravasation in atheromatous plaques ($P<0,05$ versus Q2, Figure 1C), the phenotypic characteristics of vulnerable plaque. In contrast, these correlations were absent in fibrous atherosclerotic lesions (Figure 1D).

To further investigate the relation between Ets2 levels and inflammation in human atherosclerotic lesions, tumor necrosis factor-α (TNFα), IL6, and monocyte chemoattractant protein 1 (MCP1) levels were assessed using commercial ELISAs. Ets2 protein levels showed correlations with TNFα, IL6, and MCP1 levels (TNFα: $R=0.31$, $P=0.03$; IL6: $R=0.31$, $P=0.04$; and MCP1: $R=0.40$; $P=0.006$; Figure 2A through 2C). In contrast, Ets2 showed an inverse correlation with VEGF-A protein levels ($R=-0.22$; $P=0.05$, Figure 2D). Immunohistological analysis of serial sections shows specific expression of Ets2 in the neocapillaries of human advanced atherosclerotic plaques and in the endothelium covering the lesion (Figure 2E). Taken together, these findings point toward a possible regulatory role for Ets2 in angiogenesis, vascular integrity, and inflammatory state in vulnerable plaque.

Ets2 Expression Promotes Vulnerable Plaque Development in ApoE$^{-/-}$ Mice With Aggravated Vascularization and Intraplaque Hemorrhaging

The data obtained from the CEA human samples identified a potential function for Ets2 in regulating plaque neovascularization and inflammatory state. To further unravel Ets2 function in ECs in atherosclerosis, endogenous Ets2 protein expression was assessed in the endothelium of ApoE$^{-/-}$ mice. Whole-mount en face staining of major arteries of ApoE$^{-/-}$ mice, fed on normal chow, showed low Ets2 expression levels in the endothelium. However, Ets2 expression was markedly increased once ApoE$^{-/-}$ mice were placed on a high-fat high cholesterol diet (15% (wt/vol) cocoa butter and 0.25% (wt/vol) cholesterol; Figure 3A). In addition, Ets2 mRNA levels were enhanced in murine advanced vulnerable lesions as compared with stable lesions or healthy contralateral vessels ($P<0.05$ stable and instable versus naive; †$P<0,05$ instable versus stable; Figure 3B), as shown by quantitative polymerase chain reaction (qPCR) analysis, using a mouse model for vulnerable atherosclerotic plaque formation (VP model).[19–21] Cross-sectional immunohistological analysis of murine VP validated the en face data as basal expression levels of Ets2 in carotid vessels derived from ApoE$^{-/-}$ animals on normal chow diet showed very weak Ets2 staining, which was mainly located outside the cell nuclei (Figure 3C). In contrast, Ets2 expression could be clearly detected in ECs in the murine VP lesions and colocalized with nuclear DAPI staining (Figure 3D). Ets2 expression was hardly detected in CD68+ macrophages that comprised the largest group of cells in the lesion (Figure 3E).

Ets2-specific staining was validated by immunostaining controls (Online Figure I, supplemental data). These findings suggest that Ets2-driven transcription is involved in atherosclerosis initiation and progression through the activated endothelium.

To assess in depth the function of Ets2 in advanced atherosclerosis specifically, Ets2 overexpression was induced in vessel segments with advanced atherosclerotic lesions in the earlier described murine VP model. Adenoviral transfection of Ets2 induced a 6-fold upregulation of Ets2 mRNA and 2-fold increase in Ets2 protein levels as compared with sham virus (ΔE1-Ad)-transfected animals, at 4 days after transfection (Online Figure II, supplemental data). Recombinant Ets2 was homogenously expressed throughout the carotid artery, as shown by immunofluorescent detection of Ets2 (Online Figure II, supplemental data). There was no nonspecific cross-activation of Ets-1 target genes in vitro or in vivo, demonstrated by qPCR data of transfected carotid arteries and HUVECs that showed no response in VEGFA, VEGFR2, p21^{CIP1}, matrix metalloproteinase (MMP)1, MMP9, mRNA levels after recombinant Ets2 expression (Online Figures IV and V, supplemental data).

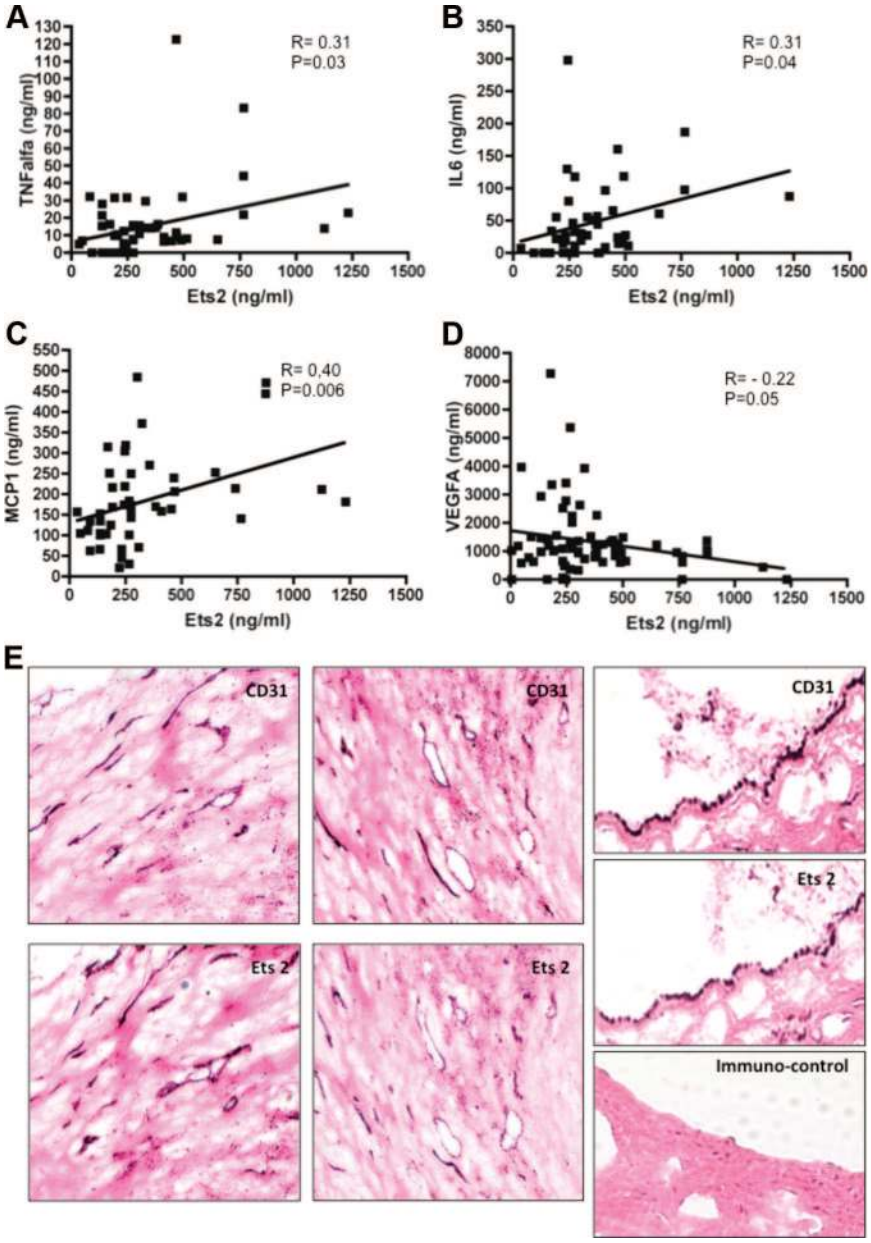

Figure 2. Rising Ets2 levels in human atherosclerotic lesions correlate with MCP1, TNFα, and IL6 and are inversely correlated with VEGFA. Positive correlations were observed between Ets2 and **A**, TNFα (R=0.31; P=0.03); **B**, IL6 (R=0.31; P=0.04); and **C**, MCP1 (R=0.40; P=0.006) in human carotid endarterectomy samples. **D**, VEGFA levels showed a negatively correlation with Ets2 (Pearson correlation, R=−0.22; P=0.05). **E**, Immunohistological staining of serial sections shows predominant expression of Ets2 in CD31+ neocapillaries in advanced human atherosclerotic lesion. First 2 panels on the left show the Ets2 and CD31 signal in the intimal neovasculature, whereas the last panel shows Ets2 and CD31 expression in the endothelium covering the atherosclerotic lesion. Primary antibodies were detected using a horseradish peroxidase–labeled secondary antibody, followed by nickel-DAP detection (brown) and eosin counterstaining. Immunostaining using matched IgG control on the same material shows limited background staining for the secondary antibody.

Ets2 expression promoted intima/media ratio of VP lesions by +130% as compared with ΔE1-Ad virus–treated animals (P<0.05; Figure 4A). In addition, Ets2 expression affected plaque phenotype: Lesions with Ets2 overexpression showed an increase in relative necrotic core size of +141% (P<0.05; Figure 4B). The relative fibrous cap thickness was decreased by −24% compared with the ΔE1-Ad group (P<0,05; Figure 4C). Ets2 expression in the atherosclerotic plaque region also increased intraplaque lipid accumulation by +89% (*P<0.05; Figure 4D) and CD68+ macrophage accumulation by +46% (*P<0.05; Figure 4E), compared with ΔE1-Ad–transfected controls. Finally, Ets2 expression diminished VSMCs content by −41% (P<0.05; Figure 4F), whereas collagen formation in the plaque remained unchanged compared with the ΔE1-Ad group (P=0.70; Figure 4G), as analyzed using a circular polarization filter set.

To further validate the angiogenic function of Ets2 that was implied by the positive correlation between Ets2 levels and intraplaque capillary density in the CEA lesions, microvessel formation in the murine VP was assessed. Indeed, Ets2 increased microvessel formation in VP lesions by +32% (P<0,05; Figure 5A) as compared with control animals. To verify the role of Ets2 in intraplaque perivascular hemorrhaging (IPH), which was suggested by the human CEA study, the murine VP lesions were assessed for intimal accumulation of erythrocytes. Ets2-Ad–transfected ApoE$^{-/-}$ mice showed a significant increase in IPH, as detected by Ter119 erythrocyte immunostaining throughout the atherosclerotic lesions (P<0,05; Figure 5B). The intraplaque Ter119 signal was mainly located outside the neovasculature of Ad-Ets2–treated murine lesions (Figure 5C). In addition, in line with the findings in human CEA, MCP1 and IL6 mRNA levels were upregulated in response to Ets2 expression in the carotid artery (Online Figure IV, supplemental data). These findings in the murine VP model demonstrate that Ets2 advances vulnerable plaque development.

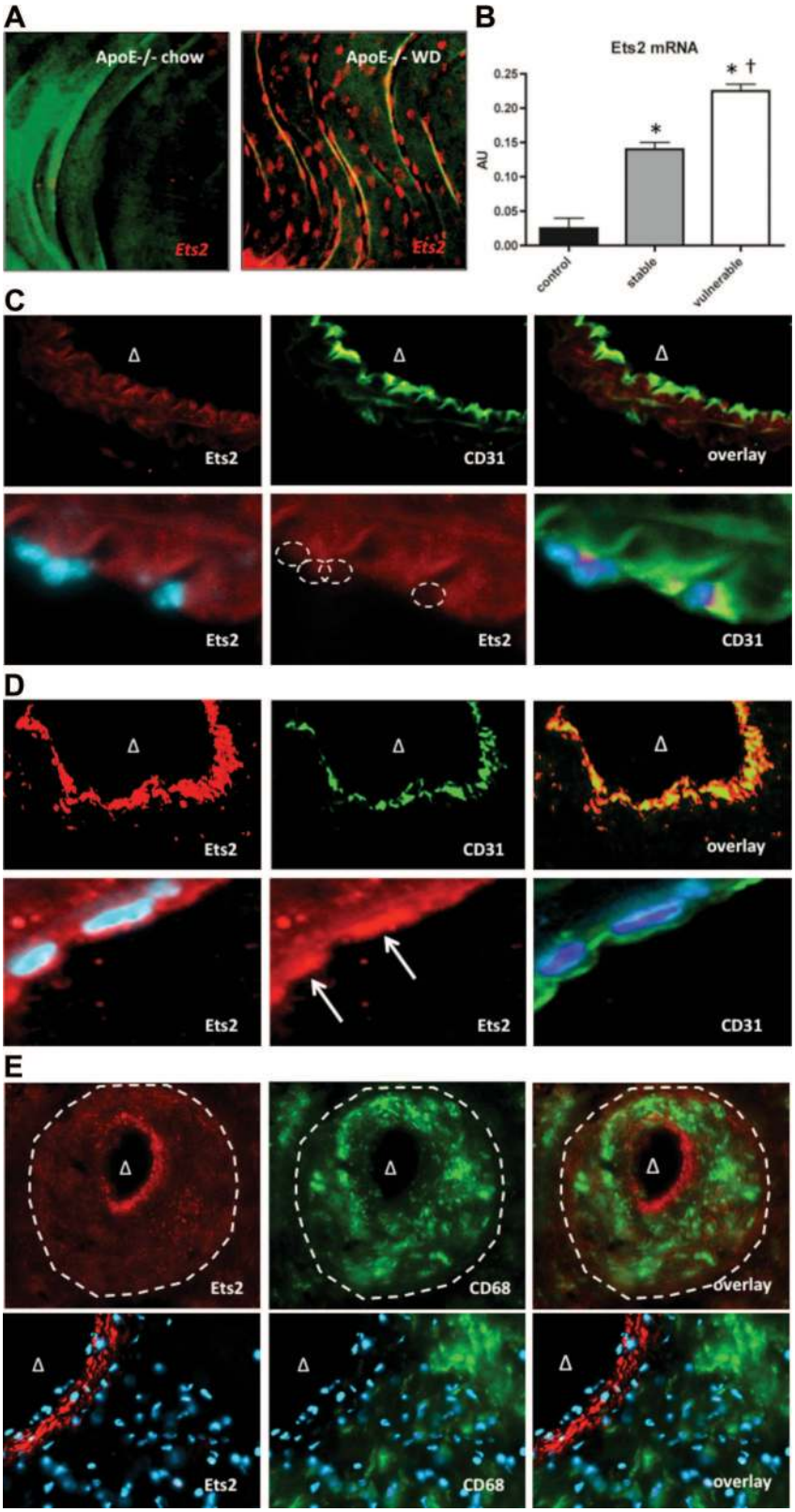

Figure 3. Endogenous expression of Ets2 in ApoE$^{-/-}$ mice. A, Endothelial Ets2 expression in aortic segments of C57bl/6 ApoE$^{-/-}$ mice that received normal chow (ApoE$^{-/-}$ chow) versus cholesterol-rich, high-fat diet for 3 weeks (ApoE$^{-/-}$ Western Diet [WD]), as assessed by whole-mount en face immunostaining and subsequent visualization of the samples using fluorescent confocal microscopy. Red fluorescence indicates the Ets2 immunofluorescent signal, and green fluorescence is due to autofluorescence of the basal elastic lamina. Representative samples of one experiment with 5 animals per group are shown. **B**, qPCR analysis showed endogenous Ets2 mRNA level in lesions with the vulnerable phenotype, compared with the contralateral naive carotid arteries and stable plaques in a mouse ApoE$^{-/-}$-based model of VP at week 9 (n=6 per group; *P<0.05 versus control. †P<0.05 versus stable). **C**, Cross-sectional immunohistological analysis in carotid vessels derived from ApoE$^{-/-}$ animals on normal chow diet showed very weak Ets2 staining. High magnification of the endothelium demonstrated that intracellular Ets2 was mainly located outside the cell nuclei. Areas of nuclei are marked with an open circle. **D**, Ets2 expression was clearly detected in CD31+ ECs in murine VP lesions and colocalized with nuclear DAPI staining (indicated by white arrows). **E**, In contrast colocalization of Ets2 (red fluorescent signal) with CD68+ (green fluorescent signal) macrophages in the lesion was limited. Dotted white lines mark the boundary between intima and media. Δ indicates lumen area.

Regulation of Ets2 Expression and Angiogenic Function in Endothelial Cells by the Proatherogenic Cytokine TNFα

To unravel the molecular mechanism by which Ets2 propagates neovascularization and IPH in advanced human and murine atheromatous lesions, we sought to define the decisive factors in atherosclerosis that are responsible for the rise in Ets2 expression in VP. Stimulation of HUVEC with different doses of LDL or oxLDL did not alter Ets2 expression levels (qPCR analysis, Figure 6A and 6B). No response was also

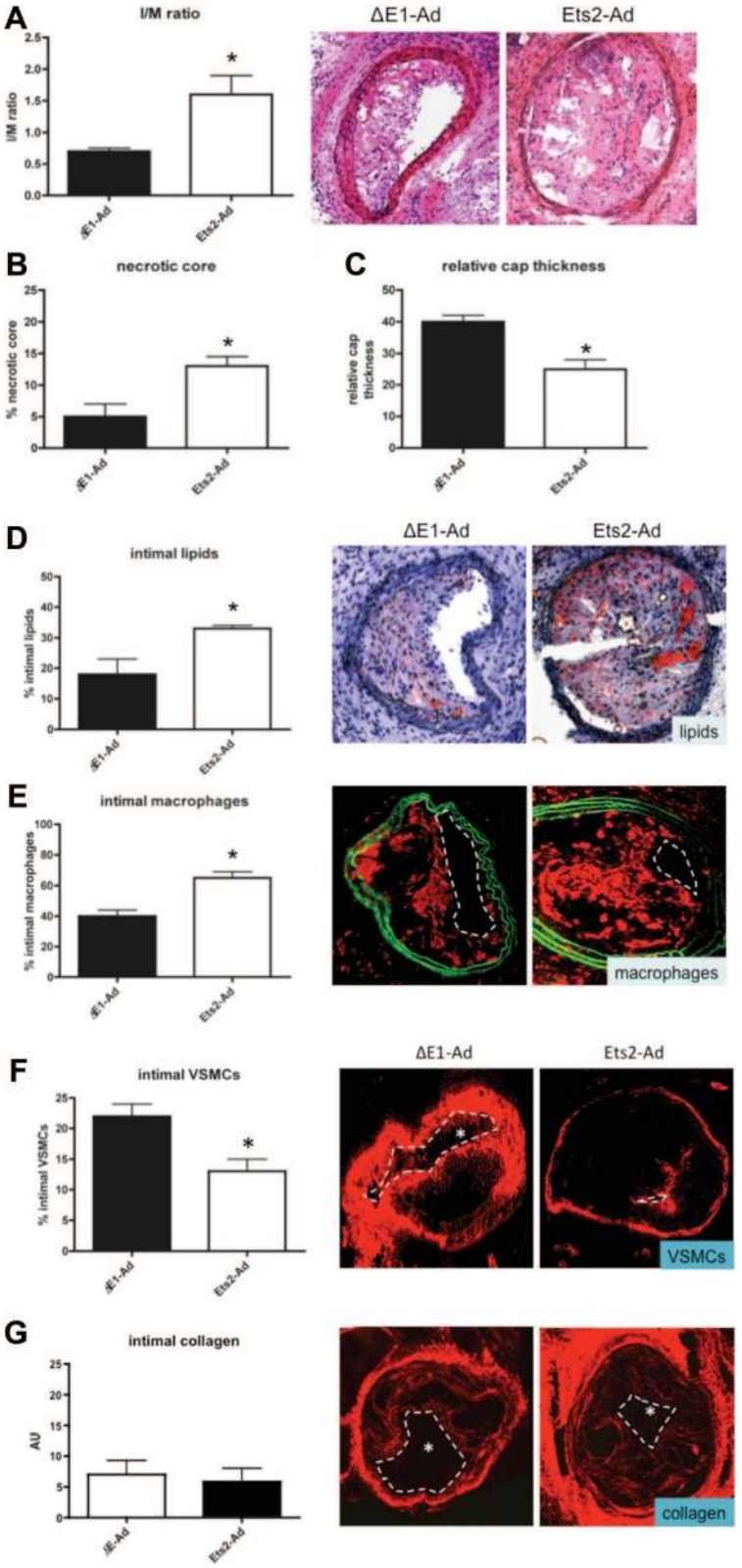

Figure 4. Overexpression of Ets2 destabilizes VP. Morphometric and immunohistological analysis of VPs in ApoE$^{-/-}$ mice that were transfected with ΔE1-Ad or Ets2-Ad, 9 weeks after VP induction. **A** through **C**, In the right column, representative cross-sections are shown. In the left column, bar graphs show the effects of Ets2 transduction on **A**, intima/media (I/M) ratio; **B**, % necrotic core (necrotic core area/intima area*100%); and **C**, relative cap thickness (ie, mean cap thickness at plaque shoulders and midregion/ maximal intimal thickness) in vulnerable lesions of ΔE1-Ad, as compared with Ets2-Ad–transfected ApoE$^{-/-}$ mice. **D** through **G**, Morphometric and immunohistological analysis of VPs in ΔE1-Ad–transfected or Ets2-Ad–transfected ApoE$^{-/-}$ mice. In the right column, representative cross-sections are shown. In the left column, bar graphs show the effects of Ets2 transduction on **D**, % intimal lipids; **E**, % intimal CD68+ macrophages; **F**, % intimal VSMCs; and **G**, % intimal collagen, in vulnerable lesions of ΔE1-Ad–transfected as compared with Ets2-Ad–transfected ApoE$^{-/-}$ mice (n=10 for each group; *$P<0.05$ versus ΔE1-Ad.) In the photographs, dotted lines indicate the luminal area. In the micrographs showing VSMC-actin or CD68 staining, the green fluorescent signal represents the autofluorescence of the elastic laminas.

observed in HUVEC cultures exposed to low oxygen conditions (21% versus 3% O_2, Figure 6C). However, stimulation of HUVECs with TNFα, a proinflammatory cytokine associated with increased plaque vulnerability that correlated with Ets2 levels in human CEA study, induced a dose-dependent upregulation of Ets2 mRNA and protein levels (Figure 6D and 6E). Simultaneously, TNFα stimulation of HUVECs induced Ets2 activation indicated by increase of Ets2 phosphorylation at Thr72 and visible nuclear translocation of this cotranscription factor (Figure 6F and 6G).

To validate the angiogenic potential of Ets2, in vitro tube formation experiments with HUVECs were conducted. Si-

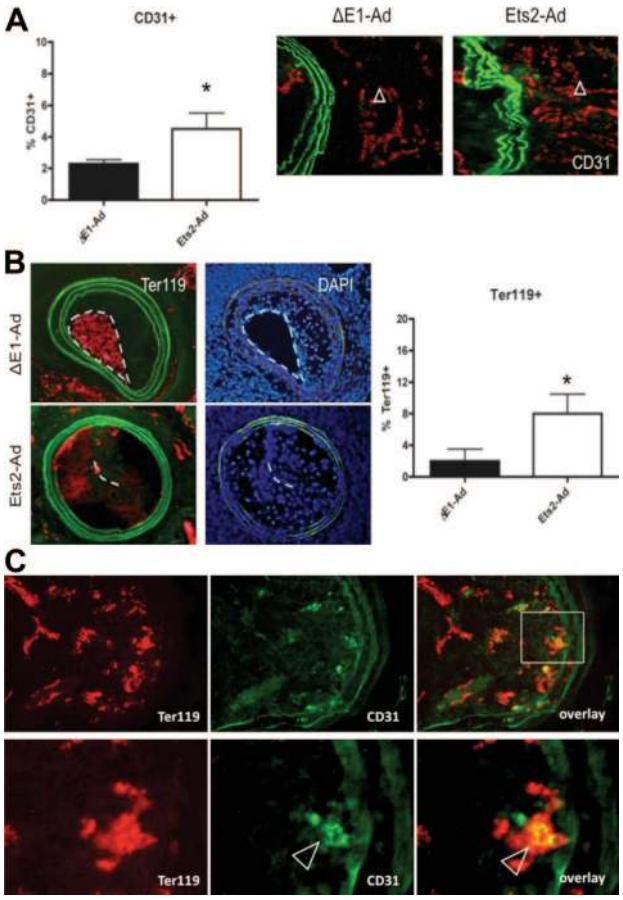

Figure 5. Ets2 expression promotes new vessel formation and intraplaque hemorrhaging in vulnerable plaque. Immunohistological analysis of VPs in ApoE$^{-/-}$ mice that were transfected with ΔE1-Ad or Ets2-Ad, 9 weeks after VP induction. **A**, Representative cross sections and bar graphs show the effects of Ets2 transduction on the % of adventitial CD31+ ECs. In the photograph panel, the green fluorescent signal represents autofluorescence from the elastic lamina, and the white triangle symbol indicates the adventitial side (n=10 for each group; *P<0,05 versus ΔE1-Ad). **B**, Micrographs show representative immunohistological staining of Ter119 (red) to identify IPH in the VP area. Nuclei are identified by DAPI (blue fluorescent signal). The green fluorescent signal represents the autofluorescence of the elastic laminas. Lumen boundaries are marked by a white dotted line. Bar graph shows the effect of adventitial Ets2 transduction on vascular integrity by scoring IPH defined as the % of Ter119+ intimal areas (n=10 for each group; *P<0.05 versus ΔE1-Ad), **C**, High-magnification micrographs of these murine lesions clearly identify Ter119+ (red fluorescent signal) erythrocytes located outside CD31+ vascular structures (green fluorescent signal) as a result of erythrocyte extravasation during intraplaque hemorrhaging. The white open arrow points out an intimal microvessel with open lumen.

lencing efficiency was validated by qPCR (Online Figure II, supplemental data). SiRNA silencing of Ets2 markedly impeded neocapillary formation in matrigel with a reduction in the number of capillary tubes, junctions, as well as total tube length, whereas the average length per tube was in decline as compared with cultures transfected with an equimolar of scrambled, nontargeting siRNA (5 ng/1×10^6 cells, 3 days after transfection, P<0,05; Online Figure III, A through E, supplemental data). Stimulation with the proatherogenic cytokine TNFα reduced total tube length and average length per tube but did not change the number of tubes or junctions (P<0.05; Online Figure III, A through E, supplemental data). Silencing of Ets2 augmented TNFα-induced attenuation of tube formation, which suggests that Ets2 acts downstream of TNFα receptor interaction (P<0.05; Online Figure III, A through E, supplemental data). Further assessment of the transcriptional profile of Ets2 siRNA silencing in ECs indentified significant downregulation of proangiogenic genes, including HO-1, EphB4, EphrinB2, DLL4, Jagged1, and Ang-2, whereas the mRNA levels of Ang-1, VEGFA, and VEGFR2 remained unaffected (Figure 6H). These data point toward TNFα as a potent atherogenic factor that drives expression and proangiogenic function of Ets2 during intimal neovascularization.

Ets2 Drives Expression of the Proatherogenic Cytokines MCP1 and IL6 and the Adhesion Molecule VCAM1 in Endothelial Cells

The positive relation between Ets2 levels and the inflammatory cytokines TNFα, IL6, and MCP1, as observed in human atherosclerotic lesions, could trigger monocyte adhesion to the luminal and adventitial microvascular endothelium, thereby promoting lesion growth and inflammatory state. We investigated the transcriptional regulation of Ets2 of the cytokines MCP1 and IL6, and the adhesion molecules VCAM1 and ICAM1 in HUVECs. SiRNA silencing of Ets2 impeded mRNA expression of MCP1, IL6 and VCAM1 expression, as compared with scrambled siRNA transfected cells (5 ng/1×10^6 cells, 3 days after transfection, indicated by qPCR (P<0.05; Figure 7A through 7D). On TNFα coincubation, expression of MCP1, IL6, and VCAM1 was significantly increased. siRNA silencing of Ets2 abolished this effect, suggestive that Ets2 was involved in the transcriptional regulation of MCP1, IL6, and VCAM1 downstream of TNFα receptor interaction. ICAM1 levels remained unresponsive to Ets2 silencing under basal and TNFα-stimulated conditions (P<0,05 Ets2; Figure 7A through 7D). In line with these findings, ELISA analysis showed that Ets2 silencing was associated with decreased protein levels of MCP1 and IL6 in the supernatant, as compared with sisham-transfected cells, either with or without TNFα stimulation (Figure 7E and 7F). These findings were validated in vivo, as Ets2 overexpression in murine carotid arteries induced the opposite effect and gave rise to increased mRNA levels of IL6 and MCP1 (qPCR analysis; Online Figure IV, supplemental data). Further qPCR analysis of the transfected cells showed that there was no cross-activation of the Ets1 target genes MMP1, MMP9, p21^{CIP1}, and Ets1, validating the functional specificity of Ets2 (Online Figure IV, supplemental data). These data point toward a role of Ets2 in regulating the inflammatory state of ECs that could define atherosclerotic lesion growth and promote further development into vulnerable plaque.

Ets2 Induces Loss of Integrity of Endothelial Monolayers in Response to TNFα In Vitro

To specify the mechanism by which Ets2 induced increased IPH, confluent endothelial monolayers of HUVECs transfected with ΔE1-Ad and Ets2-Ad were cultured on nontransparent 0.4-μm pore filters, followed by measurement of transwell endothelial leakage for 40-kDa dextran-FITC in the

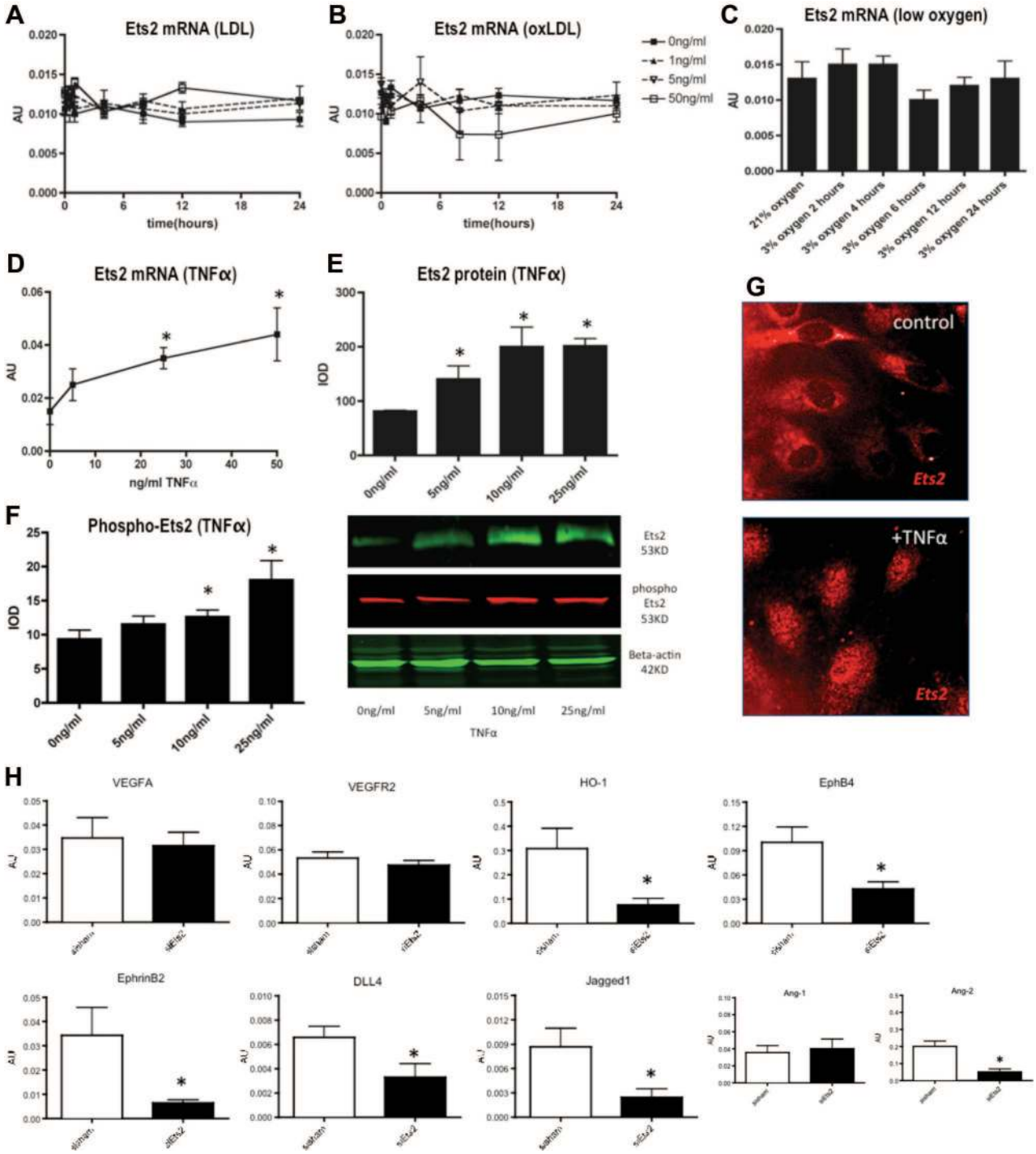

Figure 6. Ets2 responds to TNFα stimulation and promotes gene expression of angiogenic regulators in ECs. A, Endogenous Ets2 mRNA levels in HUVECs were not responsive to different doses of LDL (range, 0 to 50 μg/mL), or **B**, oxLDL (range, 0 to 50 μg/mL) as assessed by qPCR at different time points. **C**, Similarly hypoxia failed to induce Ets2 expression (normal oxygen, 21% O_2 versus low oxygen 3% O_2). **D**, TNFα stimulation (range, 0 to 50 ng/mL) induced a dose-response in Ets2 mRNA expression (n=4; *P<0,05 versus 0 ng/mL TNFα); **E**, total Ets2 protein levels (n=3; *P<0,05 versus 0 ng/mL TNFα); and **F**, Ets2 phosphorylation at the Thr72 activation site (n=3; *P<0,05 versus 0 ng/mL TNFα) after 24-hour stimulation. **G**, Stimulation of HUVECs with 25 ng/mL TNFα for 24 hours triggered translocation of Ets2 from the perinuclear compartment to the nucleus, as demonstrated by immunofluorescent staining and subsequent analysis by confocal microscopy. Shown in the figure are representative samples of 3 different experiments. Red indicates the Ets2 immunofluorescent signal. **H**, qPCR analysis of HUVECs transfected with Ets2 targeting siRNA showed reduction in expression levels of proangiogenic genes, including HO-1, EphB4, EphrinB2, DLL4, and Jagged1, whereas expression of VEGFA and VEGFR2 were not affected. In addition, angiopoietin (Ang) 2 was downregulated by Ets2 silencing, whereas Ang 1was not affected (n=5, *<0.05 versus sisham).

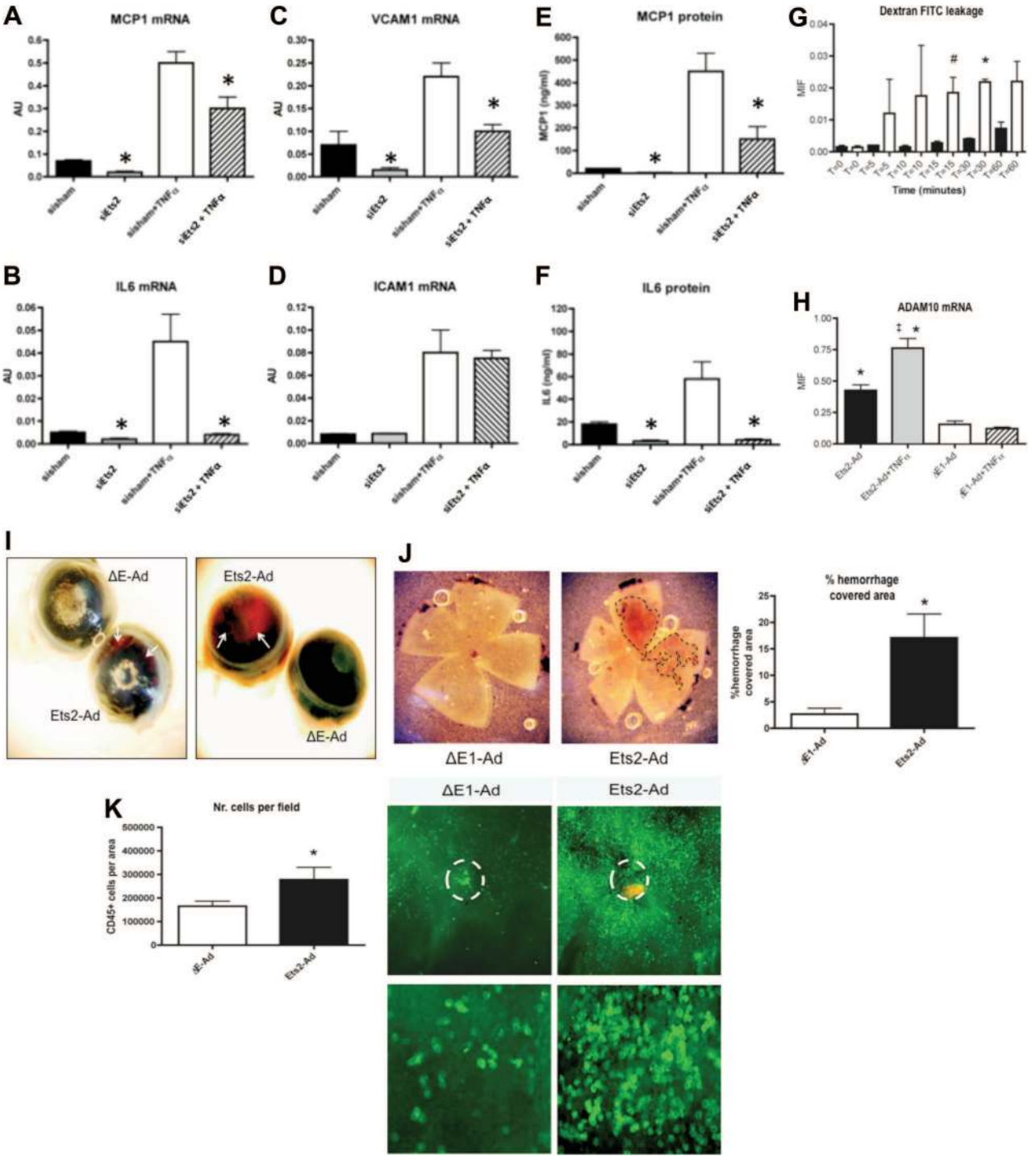

Figure 7. Ets2 regulates expression of proinflammatory cytokines and adhesion molecules and compromises endothelial integrity. qPCR analysis of MCP1, IL6, VCAM1, and ICAM expression in response to Ets2 silencing at basal levels and in response to TNFα stimulation after 24 hours. SiRNA-mediated silencing of Ets2 inhibited expression of **A**, MCP1; **B**, IL6; and **C**, VCAM1, whereas **D**, ICAM1 expression, was not affected, as compared with nontargeting scrambled siRNA transfected controls (sisham). **A** through **D**, Stimulation with 25 ng/mL TNFα increased the expression of MCP1, IL6, VCAM1, and ICAM1. Ets2 silencing similarly inhibited the response of MCP1, IL6, and VCAM1 to TNFα stimulation, whereas ICAM1 remained unaffected. **E**, Basal IL6, and **F**, MCP1 protein levels in the supernatant were decreased by Ets2 silencing, as demonstrated in dedicated ELISA assays. Stimulation with 25 ng/mL TNFα increased IL6 and MCP1 protein levels, and Ets2 silencing inhibited the response of IL6 and MCP1 to TNFα (qPCR data, n=4, ELISA data, n=6; *$P<0.05$ versus sisham or sisham+TNFα). Ets2 overexpression resulted in loss of endothelial integrity. **G**, Measurement of Dextran-FITC leakage through a monolayer of ΔE1-Ad or Ets2-Ad transfected HUVECs with or without TNFα stimulation. Graphs show mean intensity of fluorescence (*Y*-axes) of dextran-FITC measured in the lower compartment in response to 25 ng/mL TNFα in minutes (*X*-axes). Black bars indicate the response of ΔE1-Ad and white bars indicate Ets2-Ad transfected HUVEC monolayers (n=3, #$P<0.1$ versus ΔE1-Ad, *$P<0.05$ versus ΔE1-Ad). **H**, qPCR analysis of ADAM10 expression in response to Ets2 overexpression in HUVECs at basal levels and after 24-hour stimulation of 25 ng/mL TNFα (n=4 experiments, *$P<0.05$ versus ΔE1-Ad and ΔE1-Ad+TNFα, ‡$P<0,05$ versus Ets2-Ad). Ets2 overexpression in the retina of ApoE$^{-/-}$ mice promoted vascular leakage. **I**, Three days after intravitreal injection

lower chamber in the presence of either 25 ng/mL TNFα or 2 μg/mL thrombin. Baseline levels of leakage of dextran-FITC remained low in unstimulated HUVECs both in Ets2-expressing cells and control cells. However, Ets2 expression significantly amplified the dextran-FITC signal by maximal 4-fold in response to TNFα (Figure 7G) or thrombin (data not shown), as compared with ΔE1-Ad–infected cells, indicating that Ets2 augmented TNFα (and thrombin)-induced leakage of the endothelial monolayer. Loss of vascular integrity could be due to VE-cadherin shedding, a process mediated by ADAM10, a metallopeptidase prominent in the atherogenesis. ADAM10 mRNA levels assessment by qPCR revealed that Ets2 expression indeed induced a 2.5-fold upregulation of ADAM10, as compared with ΔE1-Ad transfected HUVECs. Ets2 expression further amplified TNFα-stimulated ADAM10 expression by 4-fold (Figure 7H). A similar effect was observed with thrombin stimulation (data not shown). These data identify Ets2 as an important regulator of endothelial leakage in response to proinflammatory stimuli.

Ets2 Overexpression Leads to Vascular Leakage and Leukocyte Infiltration In Vivo in the Retinal Vasculature of ApoE$^{-/-}$ Mice

To further validate our findings of Ets2-induced hemorrhaging in the murine VP model, Ets2 overexpression was induced by intravitreal injection of Ets2-Ad in mature ApoE$^{-/-}$ mice, and the effect on vascular integrity was assessed 2 days after transfection. Ets2 overexpression in the murine retina induced severe hemorrhaging in response to intravenous thrombin injection, starting from the boundary areas closest to the lens, where the choroid and the retina layers begin to overlap, spreading further out to the anterior and vitreous eye chamber (Figure 7I). In contrast, the eyes injected with sham virus did not show any response. Dissection from the choroid layer and closer examination followed by quantification of the retina revealed large patches of thrombi in the eyes treated with Ets2-Ad as compared with sham-treated samples (Figure 7J). Similarly, we used this eye model to assess the effect of Ets2 overexpression on leukocyte adhesion to validate the role of Ets2 in immune-regulation. Whole-mount en face staining for CD45+ leukocytes revealed prominent leukocyte infiltration in Ets2-Ad treated eyes as compared with sham-treated controls (Figure 7K).

These findings in the murine retinal model demonstrate that Ets2 could compromise vessel integrity by promoting vascular leakage in response to inflammatory stimulation, thereby enhancing leukocyte adhesion.

ShRNA-Mediated Ets2 Silencing Stabilizes Vulnerable Plaque Morphology in ApoE$^{-/-}$ Mice

To validate the effects of Ets2 overexpression on VP phenotype, we conducted a second series of experiments in which we silenced endogenous Ets2 expression in the murine lesions. Ets2 silencing was induced in vessel segments with advanced atherosclerosis in the murine VP model by lentiviral transfection of an shRNA construct that targets Ets2. LV-siEts2 silencing induced a -50% downregulation of Ets2 mRNA levels as compared with vessels transfected by a control nontargeting shRNA-lentiviral construct or nontransfected controls, at 4 days after transfection in murine carotid vessels (Figure 8A).

Ets2 silencing in murine VP impeded the intima/media ratio of these lesions by -55% and -50% as compared with LV-sisham or control animals, respectively (Figure 8B). Ets2 silencing also affected plaque phenotype: Lesions transfected with LV-siEts2 showed a decrease in relative necrotic core size of -83% versus LV-sisham and control animals (Figure 8C). The relative fibrous cap thickness was increased by $+64\%$ and $+87\%$ as compared with LV-sisham and control animals, respectively (Figure 8D).

Ets2 silencing further stabilized these advanced lesions, indicated by a reduction in intimal CD68+ macrophage by -55% and -59% (as compared with LV-sisham or control animals, respectively), whereas lipid deposition was not affected (Figure 8E and 8F). In contrast, Ets2 silencing increased plaque stabilization by promoting intraplaque VSMC accumulation by $+194\%$ and $+99\%$ as compared with LV-sisham and control, respectively, whereas collagen levels remained comparable to the controls (Figure 8G and 8H).

Furthermore, Ets2 silencing decreased microvessel formation in VP lesions by -88% and -79%, which coincided with a decline in intraplaque Ter119 area of -76% and -73% as compared with LV-sisham or control animals (Figure 8I and 8J).

Discussion

The current study provides evidence for a central role for Ets2 in the development of a proatherogenic endothelial cell phenotype by stimulating expression of inflammatory cytokines that could subsequently contribute to intraplaque microvessel formation with concomitant loss of vascular integrity.

The initial clinical study of human CEA identified Ets2 as a potential biomarker for the extent of neovascularization and intraplaque hemorrhaging in advanced human atheromas. This coincided with a correlation between rising intraplaque levels of Ets2 and atherogenic inflammatory markers, including TNFα, IL6, and MCP1. Based on the role of Ets2 as a potent transcriptional regulator of inflammatory cytokines,[17,18] and the observation that Ets2 is upregulated in the Flk1+ angioblasts during vascular development in mice and zebra fish, we hypothesized that Ets2 could have a proatherogenic function in advanced atherosclerotic plaque development.

Our data demonstrated that Ets2 is upregulated in the vascular endothelium of ApoE$^{-/-}$ animals in response to a high cholesterol diet. In addition, Ets2 mRNA levels were in particular upregulated in the endothelium of murine vulnerable lesions, as compared with the endothelium of healthy vessels or

Figure 7 (Continued). of Ets2-Ad or ΔE-Ad, Ets2-Ad–transfected eyes show severe hemorrhaging (indicated by arrows), whereas the eyes injected with sham virus was unresponsive. **J**, Dissection of the retina reveals an increase in areas with blood accumulation. Bar graph shows quantification of the hemorrhage area, indicated in the micrograph by a broken line (n=6 animals, *$P<0.05$ versus ΔE1-Ad and ΔE1-Ad). **K**, Representative figure of CD45+ leukocyte infiltration (green fluorescent signal) in the retina in the Ets2-Ad and sham virus–treated group. The broken line indicates the neural plexus. Magnification $\times$10 and $\times$20 was used in the **upper panel** and **lower panel**, respectively. Bar graph shows the quantification of the number of CD45+ leukocytes per microscopic field ($\times$10).

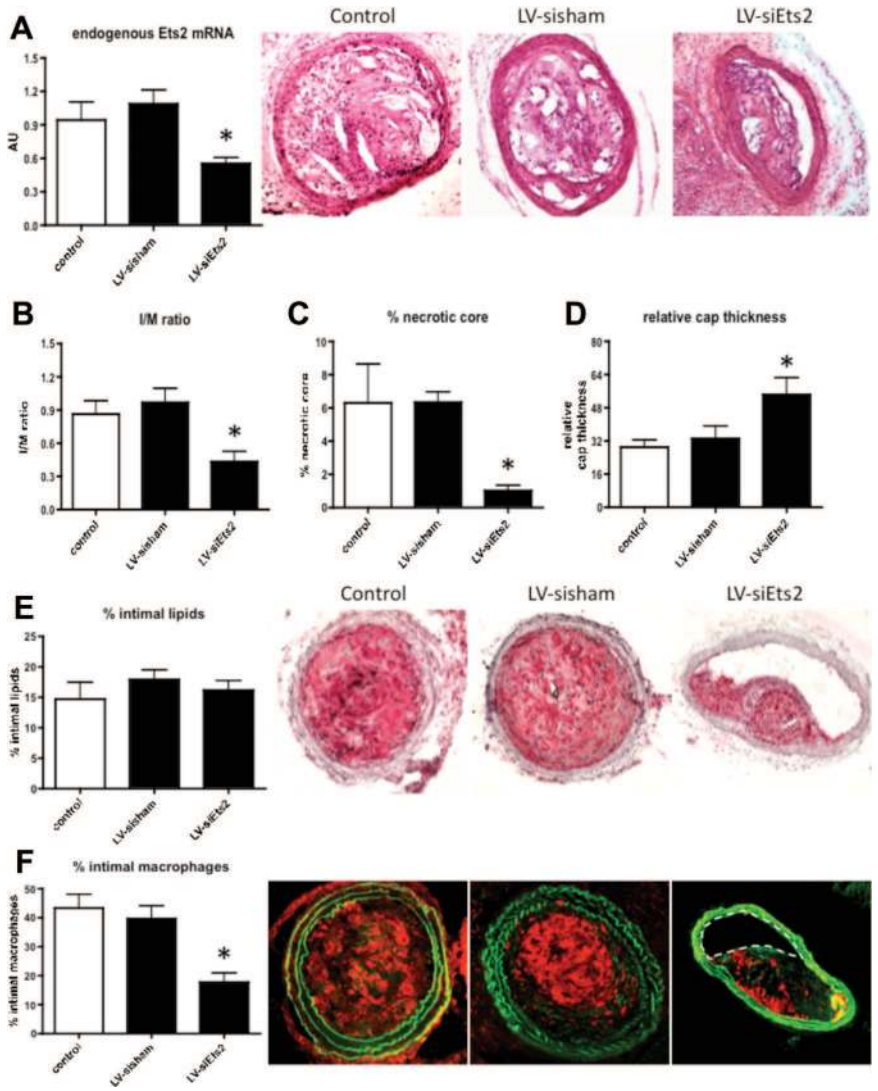

Figure 8. Ets2 silencing by shRNA promotes vulnerable plaque stabilization. Morphometric and immunohistological analysis of VPs in ApoE$^{-/-}$ mice that were transfected with a lentiviral construct that expresses Ets2 targeting shRNA (LV-siEts2) or a control lentiviral construct that expresses nontargeting shRNA (LV-sisham), 9 weeks after VP induction. **A**, qPCR assessment of endogenous Ets2 mRNA expression in LV-siEts2–transduced carotid vessel segments of ApoE$^{-/-}$ mice as compared with LV-sisham–treated animals and untreated contralateral carotid arteries after 4 days of transfection (*$P<0.05$ versus control and LV-sisham; n=4 for qPCR assessment; *$P<0.05$ versus control). **B** through **J**, Representative cross sections and bar graphs show the effects of shRNA-mediated silencing of Ets2 on **B**, intima/media (I/M) ratio; **C**, % necrotic core (necrotic core area/intima area*100%); and **D**, relative cap thickness (ie, mean cap thickness at plaque shoulders and midregion/ maximal intimal thickness) in vulnerable lesions of LV-sisham, as compared with LV-siEts2 transfected ApoE$^{-/-}$ mice. **E** through G, Analysis of plaque phenotype show the effects of Ets2 silencing on **E**, % intimal lipids; **F**, % intimal CD68+ macrophages; **G**, % intimal VSMCs; and **H**, and % intimal collagen, in vulnerable lesions of LV-sisham as compared with LV-siEts2 transfected ApoE$^{-/-}$ mice (n=8 for each group; *$P<0.05$ versus LV-sisham). In the photographs, dotted lines indicate the luminal area. In the micrographs that show VSMC-actin or CD68 staining, the green fluorescent signal represents the autofluorescence of the elastic lamina. Representative cross sections and bar graphs show the effects of Ets2 silencing using a lentiviral siRNA construct on vascularization and intraplaque hemorrhaging: **I**, The % of intimal CD31+ ECs, and **J**, % of IPH in ApoE$^{-/-}$ mice transfected with LV-sisham or LV-siEts2. Representative micrographs of CD31 and Ter119 staining are shown. For Ter119, nuclei are identified by DAPI (blue fluorescent signal), and lumen boundaries are marked by a white dotted line (n=8 for each group; *$P<0.05$ versus LV-sisham).

stable atherosclerotic lesions. In vitro experiments to pinpoint the proatherogenic stimulus for Ets2 upregulation in advanced lesions identified TNFα as a potent factor that enhanced mRNA and protein levels of Ets2 in primary human ECs in culture.

Although the Ets2 correlation data in human atheromas gave an indication that Ets2 might be involved in VP formation, it did not demonstrated in a cause-effective way that Ets2 function could directly affect disease development. To fully understand the role of Ets2 in VP pathogenesis, we conducted in vivo experiments in which we induced Ets2 overexpression in a murine VP model. Ets2 overexpression promoted lesion growth and induced progression of advanced lesions into a VP phenotype. This was marked by an increase of necrotic core and macrophage-covered area, a decrease in fibrous cap thickness, and a loss of VSMC content. More importantly, the formation of leaky microvessels formation was promoted, as identified by an increase in microvessels and hemorrhaging in the atherosclerotic area. In contrast, Ets2

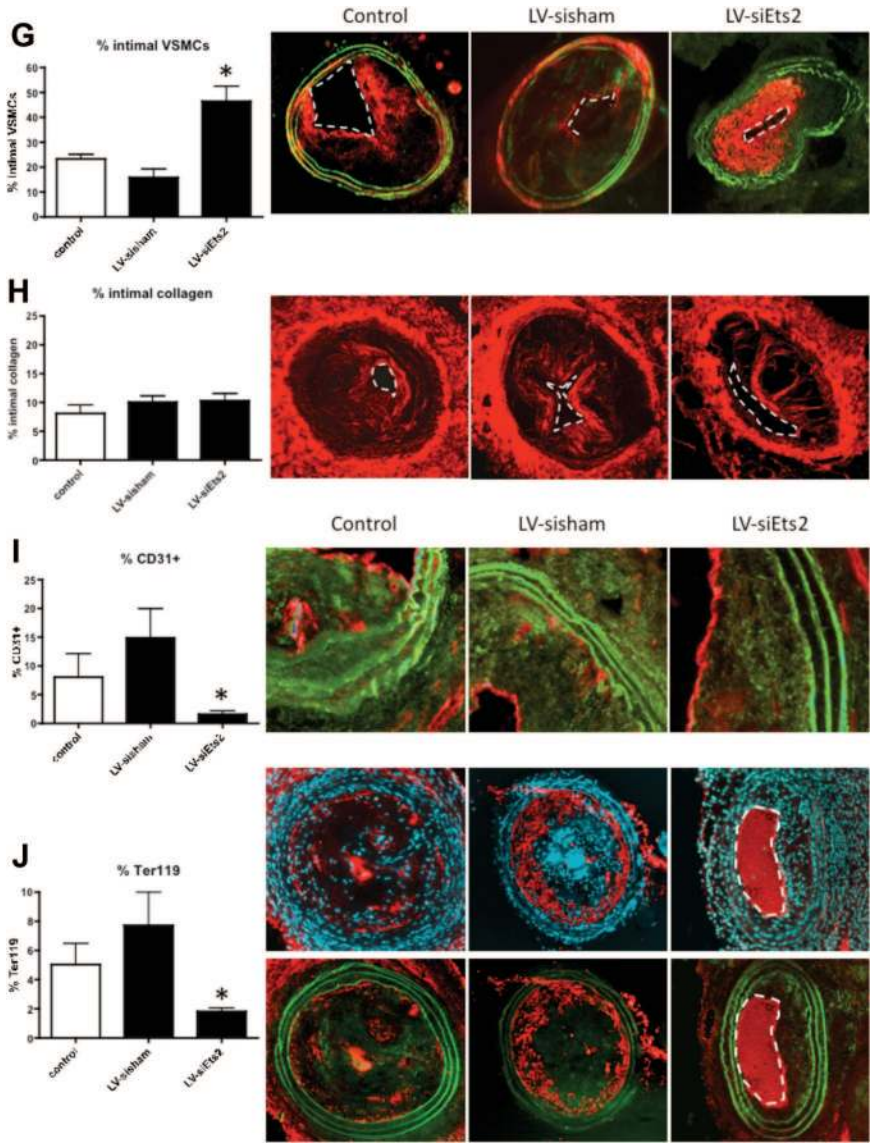

Figure 8 (Continued).

silencing induced the opposite effect and was shown to stabilize the murine VP lesions. Together, these data point toward a destabilizing function for Ets2 in the advanced lesions.

Further experiments were conducted to unravel the working mechanism of Ets2 in ECs during VP progression. Based on our findings, we propose the following mechanism by which Ets2 in ECs could affect the stability of atherosclerotic lesions: In early advanced lesions, the proinflammatory cytokine (TNFα)-rich environment triggers Ets2 expression. Ets2 functions as a modulator and amplifier of the endothelial inflammatory response via transcriptional activation of IL6, MCP1, and VCAM1, which promotes accumulation of inflammatory cells and thus heighten the inflammatory state of the atherosclerotic lesion. As suggested by our in vitro findings, Ets2 could potentially promote further lesion destabilization by directly effecting EC function, promoting vessel leakage and expansive neovascular growth from the adventitia into the intimal area, which supplies a second entry route for inflammatory cells. However, the observed effect of Ets2 on plaque stability could also predominantly be the result of the increased inflammatory state of the vulnerable lesion, which would also affect neovessel growth and IPH.

Ets2 has been shown to be involved in the transcriptional activation of angiogenic growth factors, including HO-1,[15] VEGFR1,[14] and CD13/APN.[16] In the present study, we further examined the angiogenic potential of Ets2 in vitro and in vivo. Our findings suggested that Ets2 promoted microvessel formation in the atherosclerotic region and caused subsequent plaque destabilization. Previously, animal studies have indicated that angiogenic factors, including VEGFA and placental growth factor could, in addition to regulate angiogenesis during organ development, also promote atherosclerosis formation,[22,23] whereas inhibitors of angiogenesis (angiostatin, VEGF receptor-blocking antibodies) were capable in reducing plaque growth.[24,25] In addition, several studies have linked the formation of complex adventitial and intimal vascular networks to VP development.[8–10,26] In line with these findings, enhanced microvessel formation by Ets2 overexpression in the plaque region of our murine VP model was observed, whereas a significant reduction in microangiogenesis was observed in Ets2 silenced lesions. In vitro, Ets2

regulated tube formation in HUVECs and was essential in regulating the expression of HO-1, a potent proangiogenic factor.[27,28] Ets2 silencing also inhibited expression of EphrinB2, EphB4, Jagged1, and DLL4. Both DLL4/Jagged1/notch1/4 and EphrinB2/EphB4 signaling are vital regulatory pathways for angiogenesis.[29,30] In addition, Ets2 silencing downregulated Ang-2 expression, whereas Ang-1 expression remained unaffected. Previous studies have shown that Ang-2 acts as a potent autocrine antagonist of Ang-1 activation of the Tie2 receptor. Tie2 signaling mediates endothelial cell survival and vessel stabilization. Blocking of the Tie2 pathway by Ang-2 creates an endothelium that is more susceptible for vascular destabilization during an inflammatory response and promotes tumor angiogenesis.[31] Combined, these findings imply that the proangiogenic function of Ets2 might be attributed to direct regulation of these proangiogenic pathways at the level of gene transcription by Ets2.

Ets2 correlated with pathological criteria of plaque vulnerability in the murine VP model but failed to show a clear correlation in human vulnerable plaque. However, recent clinical studies have suggested that independent predictors for plaque rupture and major adverse cardiac events are intraplaque microvessel growth and intraplaque hemorrhaging (reviewed in Reference 10).[10] In this perspective, Ets2 levels in human atheroma did show a correlation with both intraplaque microvessel density and thrombogenicity, suggestive of a plaque-destabilizing role for Ets2 in the murine and human vulnerable plaques that could be attributed to inflammation-driven neovascularization in the lesions. In addition, whereas in the mouse VP study the atherosclerotic lesions were assessed at 9 weeks during early onset of vulnerable plaque, the clinical study included patients with a heterogeneous history of cardiovascular disease in which the age of atheromatous or fibrous lesions remained difficult to determine by immunohistological and morphological assessment. Ets2 expression in VP could therefore be time-dependent, and could be mainly an early determinant of plaque vulnerability, whereas Ets2 correlations with plaque vulnerability become less clear in the complex group of advanced lesions with more pleiotropic manifestations of vulnerable plaque, including postrupture lesions with a VSMC/collagen rich healed thrombus that compose the new fibrous cap, nonruptured calcified lesions, and lesions with xanthomas or advanced lesions overlaying the cap.[7]

More importantly, intraplaque microvessels often lack endothelial integrity,[8] which results in vascular leakage and perivascular accumulation of erythrocyte-derived free cholesterol in the necrotic core. The ensuing increase in macrophage infiltration and foam cell formation could propagate progression from stable into vulnerable lesion.[6,8–10,32,33] We show that Ets2 could promote loss of vascular endothelial integrity in response to TNFα stimulation, whereas Ets2 overexpression in the VP region increased intraplaque hemorrhaging. Several inflammatory mediators, including TNFα, indeed could increase vascular leakage by upregulation of the metallopeptidase ADAM10 that could induce gaps in the adherens junctions by active proteolysis of VE-cadherin.[34] However, the potential role of Ets2 in vascular growth and vessel leakage during vulnerable plaque progression should still be interpreted with discretion: Advanced atherosclerotic lesion progression is a complex, multifaceted disease, and Ets2 function, as discussed earlier, could also be primarily dependent on the regulation of Ets2 in cytokine and adhesion factor expression in ECs. Although our murine in vivo model provides unique opportunities to study the effect of Ets2 on vulnerable plaque stability, it remains difficult to separate the effects of inflammation, neovascularization and vascular integrity regulation as each of these mechanisms are so heavily intertwined in the natural process of the disease. In addition, considering the relative weak correlations that were observed between Ets2 levels and the different inflammation and lesion morphological markers of plaque vulnerability in the human samples, extrapolation of the findings in vitro and the murine model to the human disease should be discreet.

Conclusion

The current study provides first evidence for the plaque-destabilizing role of Ets2 in atherosclerosis development. Ets2 enhances the TNFα-driven inflammatory response of the endothelium, leading to a proatherosclerotic environment that promotes inflammatory infiltration and subsequent microvessel formation with compromised vascular integrity in the VP region that ultimately affects lesion stability.

Acknowledgments

We thank Pieter van Veelen, Bart Bosman, Mikel Rijken, Manisha Anandbahadoer, Hans Meijer, and Marielle Maas for excellent technical assistance.

Sources of Funding

Caroline Cheng is the recipient of a Dutch NWO-VENI grant 2008 and Erasmus fellowship grant 2010. Henricus J. Duckers is the recipient of the Dutch NWO-VIDI grant.

Disclosures

None.

References

1. Segers D, Helderman F, Cheng C, van Damme LC, Tempel D, Boersma E, Serruys PW, de Crom R, van der Steen AF, Holvoet P, Krams R. Gelatinolytic activity in atherosclerotic plaques is highly localized and is associated with both macrophages and smooth muscle cells in vivo. *Circulation*. 2007;115:609–616.
2. Schaar JA, Muller JE, Falk E, Virmani R, Fuster V, Serruys PW, Colombo A, Stefanadis C, Ward Casscells S, Moreno PR, Maseri A, van der Steen AF. Terminology for high-risk and vulnerable coronary artery plaques: report of a meeting on the vulnerable plaque, June 17 and 18, 2003, Santorini, Greece. *Eur Heart J*. 2004;25:1077–1082.
3. Schwartz SM, Galis ZS, Rosenfeld ME, Falk E. Plaque rupture in humans and mice. *Arterioscler Thromb Vasc Biol*. 2007;27:705–713.
4. den Dekker WK, Cheng C, Pasterkamp G, Duckers HJ. Toll-like receptor 4 in atherosclerosis and plaque destabilization. *Atherosclerosis*. 209:314–320.
5. Aiello RJ, Bourassa PA, Lindsey S, Weng W, Natoli E, Rollins BJ, Milos PM. Monocyte chemoattractant protein-1 accelerates atherosclerosis in apolipoprotein E-deficient mice. *Arterioscler Thromb Vasc Biol*. 1999; 19:1518–1525.
6. Moulton KS, Vakili K, Zurakowski D, Soliman M, Butterfield C, Sylvin E, Lo KM, Gillies S, Javaherian K, Folkman J. Inhibition of plaque neovascularization reduces macrophage accumulation and progression of advanced atherosclerosis. *Proc Natl Acad Sci U S A*. 2003;100:4736–4741.
7. Kolodgie FD, Virmani R, Burke AP, Farb A, Weber DK, Kutys R, Finn AV, Gold HK. Pathologic assessment of the vulnerable human coronary plaque. *Heart*. 2004;90:1385–1391.
8. Moulton KS, Olsen BR, Sonn S, Fukai N, Zurakowski D, Zeng X. Loss of collagen XVIII enhances neovascularization and vascular permeability in atherosclerosis. *Circulation*. 2004;110:1330–1336.

9. Kwon HM, Sangiorgi G, Ritman EL, McKenna C, Holmes DR, Jr., Schwartz RS, Lerman A. Enhanced coronary vasa vasorum neovascularization in experimental hypercholesterolemia. *J Clin Invest*. 1998;101:1551–1556.
10. Virmani R, Kolodgie FD, Burke AP, Finn AV, Gold HK, Tulenko TN, Wrenn SP, Narula J. Atherosclerotic plaque progression and vulnerability to rupture: angiogenesis as a source of intraplaque hemorrhage. *Arterioscler Thromb Vasc Biol*. 2005;25:2054–2061.
11. Moreno PR, Purushothaman KR, Fuster V, Echeverri D, Truszczynska H, Sharma SK, Badimon JJ, O'Connor WN. Plaque neovascularization is increased in ruptured atherosclerotic lesions of human aorta: implications for plaque vulnerability. *Circulation*. 2004;110:2032–2038.
12. Moreno PR, Purushothaman KR, Sirol M, Levy AP, Fuster V. Neovascularization in human atherosclerosis. *Circulation*. 2006;113:2245–2252.
13. Dwyer J, Li H, Xu D, Liu JP. Transcriptional regulation of telomerase activity: roles of the Ets transcription factor family. *Ann N Y Acad Sci*. 2007;1114:36–47.
14. Wakiya K, Begue A, Stehelin D, Shibuya M. A cAMP response element and an Ets motif are involved in the transcriptional regulation of flt-1 tyrosine kinase (vascular endothelial growth factor receptor 1) gene. *J Biol Chem*. 1996;271:30823–30828.
15. Chung SW, Chen YH, Perrella MA. Role of Ets-2 in the regulation of heme oxygenase-1 by endotoxin. *J Biol Chem*. 2005;280:4578–4584.
16. Petrovic N, Bhagwat SV, Ratzan WJ, Ostrowski MC, Shapiro LH. CD13/APN transcription is induced by RAS/MAPK-mediated phosphorylation of Ets-2 in activated endothelial cells. *J Biol Chem*. 2003;278:49358–49368.
17. Blumenthal SG, Aichele G, Wirth T, Czernilofsky AP, Nordheim A, Dittmer J. Regulation of the human interleukin-5 promoter by Ets transcription factors. Ets1 and Ets2, but not Elf-1, cooperate with GATA3 and HTLV-I Tax1. *J Biol Chem*. 1999;274:12910–12916.
18. Gri G, Savio D, Trinchieri G, Ma X. Synergistic regulation of the human interleukin-12 p40 promoter by NFkappaB and Ets transcription factors in Epstein-Barr virus-transformed B cells and macrophages. *J Biol Chem*. 1998;273:6431–6438.
19. Cheng C, Noordeloos AM, Jeney V, Soares MP, Moll F, Pasterkamp G, Serruys PW, Duckers HJ. Heme oxygenase 1 determines atherosclerotic lesion progression into a vulnerable plaque. *Circulation*. 2009;119:3017–3027.
20. Cheng C, Tempel D, van Haperen R, van der Baan A, Grosveld F, Daemen MJ, Krams R, de Crom R. Atherosclerotic lesion size and vulnerability are determined by patterns of fluid shear stress. *Circulation*. 2006;113:2744–2753.
21. Cheng C, Tempel D, van Haperen R, de Boer HC, Segers D, Huisman M, van Zonneveld AJ, Leenen PJ, van der Steen A, Serruys PW, de Crom R, Krams R. Shear stress-induced changes in atherosclerotic plaque composition are modulated by chemokines. *J Clin Invest*. 2007;117:616–626.
22. Celletti FL, Waugh JM, Amabile PG, Brendolan A, Hilfiker PR, Dake MD. Vascular endothelial growth factor enhances atherosclerotic plaque progression. *Nat Med*. 2001;7:425–429.
23. Celletti FL, Hilfiker PR, Ghafouri P, Dake MD. Effect of human recombinant vascular endothelial growth factor165 on progression of atherosclerotic plaque. *J Am Coll Cardiol*. 2001;37:2126–2130.
24. Moulton KS, Heller E, Konerding MA, Flynn E, Palinski W, Folkman J. Angiogenesis inhibitors endostatin or TNP-470 reduce intimal neovascularization and plaque growth in apolipoprotein E-deficient mice. *Circulation*. 1999;99:1726–1732.
25. Celletti FL, Waugh JM, Amabile PG, Kao EY, Boroumand S, Dake MD. Inhibition of vascular endothelial growth factor-mediated neointima progression with angiostatin or paclitaxel. *J Vasc Interv Radiol*. 2002;13:703–707.
26. Drinane M, Mollmark J, Zagorchev L, Moodie K, Sun B, Hall A, Shipman S, Morganelli P, Simons M, Mulligan-Kehoe MJ. The antiangiogenic activity of rPAI-1(23) inhibits vasa vasorum and growth of atherosclerotic plaque. *Circ Res*. 2009;104:337–345.
27. Cheng C, Noorderloos M, van Deel ED, Tempel D, den Dekker W, Wagtmans K, Duncker DJ, Soares MP, Laman JD, Duckers HJ. Dendritic cell function in transplantation arteriosclerosis is regulated by heme oxygenase 1. *Circ Res*. 106:1656–1666.
28. Larsen K, Cheng C, Duckers HJ. Regulation of vulnerable plaque development by the heme oxygenase/carbon monoxide system. *Trends Cardiovasc Med*. 2010;20:58–65.
29. Kume T. Novel insights into the differential functions of Notch ligands in vascular formation. *J Angiogenes Res*. 2009;1:8.
30. Cheng N, Brantley DM, Chen J. The ephrins and Eph receptors in angiogenesis. *Cytokine Growth Factor Rev*. 2002;13:75–85.
31. Thomas M, Augustin HG. The role of the angiopoietins in vascular morphogenesis. *Angiogenesis*. 2009;12:125–137.
32. Leroyer AS, Rautou PE, Silvestre JS, Castier Y, Leseche G, Devue C, Duriez M, Brandes RP, Lutgens E, Tedgui A, Boulanger CM. CD40 ligand+ microparticles from human atherosclerotic plaques stimulate endothelial proliferation and angiogenesis a potential mechanism for intraplaque neovascularization. *J Am Coll Cardiol*. 2008;52:1302–1311.
33. Cheng C, Tempel D, van Haperen R, van Damme L, Algur M, Krams R, de Crom R. Activation of MMP8 and MMP13 by angiotensin II correlates to severe intra-plaque hemorrhages and collagen breakdown in atherosclerotic lesions with a vulnerable phenotype. *Atherosclerosis*. 2009;204:26–33.
34. Schulz B, Pruessmeyer J, Maretzky T, Ludwig A, Blobel CP, Saftig P, Reiss K. ADAM10 regulates endothelial permeability and T-Cell transmigration by proteolysis of vascular endothelial cadherin. *Circ Res*. 2008;102:1192–1201.

Novelty and Significance

What Is Known?

- In atherosclerosis, the inflammatory state and extensive neovascularization in the lesion determine plaque vulnerability to rupture.
- v-ets erythroblastosis virus E26 oncogene homolog 2 (Ets2) is a cotranscription factor that regulates expression of proinflammatory and angiogenic factors.

What New Information Does This Article Contribute?

- Ets2 promotes neovascularization and intraplaque hemorrhaging in atherosclerotic lesions in mouse models of atherosclerosis.
- Ets2 activates the endothelial cells in the murine atheromatous plaque, thereby inducing expression of proinflammatory cytokines and adhesion molecules that leads to increased immune cell recruitment and a heightened inflammatory state.
- Ets2 enhances murine atheromatous plaque growth and destabilizes advanced atherosclerotic lesions in preclinical models.

Advanced atherosclerotic lesions with a thin fibrous cap and a large necrotic core are considered the culprit lesions that rupture and lead to acute thrombotic lumen occlusion in patients. As plaque vulnerability is correlated with inflammation and neovascularization, the discovery of novel genetic factors that regulate these aspects could aid in our understanding of plaque destabilization. We found that Ets2, a cotranscription factor that induces expression of a select group of target genes, actively promotes new vessel formation and inflammation in murine atherosclerotic plaques, resulting in lesion growth and destabilization. The finding links Ets2 to the process of plaque progression and extends our knowledge of potential molecular mechanisms of neovascularization in vulnerable plaque. Based on our findings, we conclude that Ets2 could function as a surrogate biomarker for plaque vulnerability to aid in clinical diagnosis of vulnerable plaques. It could also provide a future target for potent immunosuppression- and angiosuppression-based therapy in treatment of vulnerable plaque.

Supplemental Data

Material and methods

Analysis of the human atherosclerotic plaques in human CEA specimens

Atherosclerosis samples were obtained from a biobank collection of endarterectomy-derived specimens of patients that had been diagnosed with symptomatic carotid artery disease (Athero Express Biobank, University Medical Center Utrecht, The Netherlands). The study was approved by an institutional review committee, and all the subjects involved provided informed consent. Samples had been processed for immunohistological analysis, as well as protein extraction, and were quantified by two independent observers for histo-morphological indices of plaque vulnerability, as reported earlier[1]. CEA specimens are harvested, embedded in paraffin, and immunohistochemically examined for the presence of macrophages, VSMCs, collagen, endothelial cell (CD31+) and lipids. In addition, plaque thrombogenicity is assessed by the presence of intraluminal thrombus or intraplaque erythrocyte deposition, in stained hematoxylin/eosin sections. In addition, adjacent sections of the collected CEA atherosclerotic plaques are freshly frozen for protein analysis. Total protein concentration was determined by a colorimetric protein assay, followed by optical spectroscopy (Biorad, The Netherlands). Protein samples of 91 patients were randomly selected from the Athero Express biobank and analyzed. Plaques were subdivided into fibrous, fibro-atheromatous, and atheromatous lesions, based on plaque morphology as assessed on hematoxylin/eosin stained sections. For analysis of plaque thrombogenicity and neovascularization, the CEA material was divided into lesions with no, minor, moderate and heavy neovascularization/thrombogenicity by scoring for the presence of CD31+

endothelial cells/erythrocytes in the intimal area. Ets2 protein levels in the lysates were assessed with the sensiflex fluorescence sandwich-ELISA detection system (Invitrogen, The Netherlands) using a rabbit anti Ets2 polyclonal antibody (Aviva, The Netherlands) for capture and a mouse anti Ets2 polyclonal antibody (Abnova, The Netherlands) for detection of the antigen. The association between Ets2 protein levels and patient CEA characteristics was analyzed using a Kruskal Wallis one-way analysis of variance for ranks, followed by a Dunn's multiple comparison test and a bonferroni correction, or a non-parametric student's T test when appropriate. Correlations between Ets2 and neovessel density or cytokine levels were tested for statistical significance using the Pearson test for correlations. Data are presented as mean ± SEM unless stated differently. P values less than 0,05 were considered significant.

Vulnerable plaque model in ApoE -/- mice

All experiments were conducted in compliance with institutional (Erasmus University Medical Center, Rotterdam, the Netherlands) and national guidelines. ApoE–/– mice (12-15 weeks, Jackson Laboratory, Bar Harbor, USA) on a Western type diet (diet W, Hope Farms, The Netherlands) were anaesthetized by isoflurane inhalation, and received a cast implantation in the right common carotid artery position. At six weeks after cast placement, animals were anaesthetized, and 50 μl of $1x10^{10}$ pfu/ml recombinant adenovirus (either Ets2-Ad or ΔE1-Ad, v/v 1:1) or lentivirus (either LV-siEts2 or LV-sisham, v/v 1:1) mixed with pluronic gel (Sigma, The Netherlands) was applied to the adventitia proximal to the cast, the predicted location of the vulnerable plaque. After an incubation time of 10 minutes, the gel was coagulated and the wound was closed. 21 days

later, the carotid arteries were harvested for histological and immuno-histochemical analysis.

Retina transfection in ApoE-/- mice

ApoE–/– mice (12- 15 weeks, Jackson Laboratory, Bar Harbor, USA) were anaesthetized by isoflurane inhalation and received intravitreal micro-injection of 2 μl of $0.5x10^{10}$ pfu/ml recombinant adenovirus (either Ets2-Ad or ΔE1-Ad). Animals were allowed to recover and were sacrificed two days post injections.

Tissue preparation and histological analysis

Carotid arteries were embedded in OCT (Sakura Finetek, the Netherlands) and snap-frozen in liquid nitrogen. Quantification of histological data was performed on sequential 5 μm cryosections at 100 μm intervals. In addition to standard hematoxylin/eosin (H/E) staining, immunohistochemical analysis included assessment of macrophages (anti-CD68 antibody, Santa Cruz Biotechnology Inc., The Netherlands), and VSMCs (anti-α-actin antibody, Sigma, Zwijndrecht, The Netherlands). Endothelial cells and intra-plaque haemorrhage (IPH) were visualized using an anti-CD31 antibody and an anti-Ter119 antibody (BD Bioscience, the Netherlands) respectively. Lipid and collagen depositions were visualized by Oil-red O and picrosirius red stainings, and collagen was subsequently imaged using a circular polarization filterset.

Ets2 was detected using a rabbit anti Ets2 polyclonal antibody (Aviva, The Netherlands). Data analysis was performed using a commercial image analysis system (Impak C, Clemex Technologies, Canada). Intima/media ratios and necrotic core/intima ratios were

analyzed in H/E-stained carotid sections. The necrotic area was defined as the neointimal area devoid of cellular tissue. Relative fibrous cap thickness was defined as the ratio of the average cap thickness at the shoulder and mid- plaque region divided by maximal intima cross-sectional thickness. The percentage of the various plaque components was calculated as the surface area positive for each specific indicatives expressed as a percentage of the total intimal surface area. Statistical analysis was performed using unpaired student's t-tests. Data are presented as mean ± SEM. P values less than 0,05 were considered significant.

En face whole mount staining

Thoracic aortic segments of ApoE-/- mice, fed on normal chow or Western type diet, were harvested following in situ perfusion at three weeks of Western Diet. Samples were overnight fixed in 4% PFA/PBS, washed in phosphate-buffered saline (PBS), and treated with 0.2% Triton X-100/PBS (Sigma Chemical, Zwijndrecht, the Netherlands). Samples were then incubated in PBS with 2.5% horse serum and 0.2% bovine serum albumin (BSA) for 30 minutes, washed and incubated overnight at 4°C with a rabbit polyclonal antibody against Ets2 (Aviva Systems, the Netherlands), followed by an incubation for 2 hours at RT with mouse anti–rabbit IgG conjugated to R594 (Molecular Probes, Leiden, the Netherlands). Sections were mounted in Vectashield (Vector Laboratories, Burlingame, USA), and examined using a confocal microscopy (LSM510LNO inverted laser scanning confocal fluorescence microscope, Carl Zeiss, Thornwood, USA). For en face staining of CD45+ leukocytes in the retina, the injected eyes were postfixed in 4%PFA/PBS, the retinas were dissected and with retina were stained following the above

protocol, with the exception that the first antibody incubation was performed using a rat anti-mouse CD45-FITC antibody (Pharmingen, The Netherlands).

Analysis of Ets2 silencing and overexpression in HUVEC culture

Primary cultures of human umbilical vein endothelial cells (HUVECs, ATCC, USA) were cultured under normoxic conditions (21% O^2) in EBM2 medium supplemented with bullet kit (EGM-2 MV Bulletkit CC-3156 & CC-4147, Lonza, the Netherlands), and 1% penecillin/streptavidin. Cell cultures with passages below 6 were used throughout the study. For Ets2 silencing, HUVECs were grown to 60% confluence, and transfected with a mix of 4 siRNAs sequences targeting Ets2 according to the instructions of the manufacturer (5 ng/1x10^6 HUVECs, transfection buffer 1, Dharmacon, Thermoscientific, the Netherlands). Equal amounts of scrambled non-targeting siRNAs were used as control. Knockdown of Ets2 expression was validated by qPCR analysis at day 2 post transfection. Cultures with <80% reduction in Ets2 RNA expression as compared to the control cultures were excluded. HUVECs were stimulated for 6 hours with TNFα (R&D systems, UK) before harvesting for qPCR or Elisa analysis. HUVECs were stimulated with several concentrations of human LDL or oxLDL (AbD SeroTech, and Thermo Scientific, the Netherlands) for 3 hours, or were cultured o/n under low oxygen conditions (3% O^2), before harvesting for qPCR analysis. For the *in vitro* permeability assay, transfected HUVECs were cultured on a non-transparent 0,4 μm pore filter inserts till they reached full confluency before they were assessed for 40KD detran-fitc leakage. The filters with monolayers were placed in a 24 wells plate, and detran-fitc leakage was measured after stimulation with either 25 ng/ml TNFα or 2 μg/ml thrombin by measuring

the fitc fluorescent signal in the supernatant of the lower chamber using a conventional Elisa plate reader at multiple time points.

qPCR and westernblot analysis

For determination of endogenous Ets2 levels in vulnerable and stable murine plaques, freshly isolated carotid arterial segments derived from cast-implanted ApoE-/- mice were divided into 2 regions (up to 0.5 mm proximal from the cast, and from 0.5 mm distal to the cast). For qPCR or westernblot analysis for the evaluation of Ets2 overexpression or silencing, the naïve carotid ateries of ApoE-/- mice were transfected with either Ets2-Ad, LV-siEts2 or lenti/adeno sham virus were used. In HUVEC cultures, cells were harvested and total RNA was extracted using the RNeasy kit (Qiagen, the Netherlands). Quality and quantity of the RNA was verified on an Agilent 2100 Bioanalyzer (Agilent Technologies, UK), and reverse transcribed. Quantitative PCR analysis was performed using an iCycler iQ Detection System (Bio- Rad, the Netherlands). Primers were designed for Ets1, Ets2, IL6, MCP1, VCAM1, ICAM1, VEGFA, VEGFR2, MMP1, MMP9, $p21^{CIP1}$, and ADAM10, and mRNA levels detected by qPCR were expressed relative to the house keeping genes, hypoxanthine guanine phosphoribosyl transferase (HPRT, for murine samples), and beta actin (for human samples). The primer sequences are provided in the supplemental data (table 1). Statistical analyses were performed using unpaired student's t-test or one-way ANOVA, when appropriate. Data are presented as mean ± SEM. P values less than 0,05 were considered significant. For western blot analysis, cell culture and tissue samples were lysed in NP40 buffer, and analyzed using SDS-PAGE western blots and 1:1000 rabbit polyclonal antibody against Ets2 (Aviva Systems, the

Netherlands). Protein bands were visualized using the Li-Cor detection system (Westburg, The Netherlands), as previously described, using beta-actin as a loading control[1].

Elisa analysis of protein expression

Cellular proteins were extracted using NP-40 lysis buffer (150 mmol/L NaCl, 50 mmol/L Tris (pH 8.0), and 1% Nonidet P-40). Total protein concentration was determined by a colorimetric protein assay, followed by optical spectroscopy (BioRad, the Netherlands). IL6 and MCP1 protein expression levels in cell lysates were assessed with a commercial quantitative sandwich Elisa assays following the manufacturer's instructions (mouse IL6 and mouse MCP1 Elisa kit are both from Bender MedSystems, Germany). Statistical analysis was performed using one-way ANOVA. Data are presented as mean ± SEM. P values less than 0,05 were considered significant.

Tube Formation Assays

In vitro formation of tube structures was studied on BioCoat Matrigel tissue culture plates (BD Biosciences, The Netherlands). SiRNA transfected HUVECs were plated at 30000 cells/well in 96-well plates precoated with a solution of Matrigel basement membrane matrix. After 24 hours of incubation at 37°C, cells were visualized by Calcein-Am uptake (BD biosciences, The Netherlands) tube organization was examined using an inverted fluorescence microscopy, and the photographs were subsequently analyzed using the commercial image analysis system (AngioSys,UK). Statistical analysis was performed

using one-way ANOVA. Data are presented as mean ± SEM. P values less than 0,05 were considered significant.

Primer sets used for qPCR analysis

Primer set	antisense	sense
Human Ets2	GCAGATTCACGTTCACCAGA	GCAAGGCTGGTATGAGTCAA
Human βactin	AGCACTGTGTTGGCGTACAG	TCCCTGGAGAAGAGCTACGA
Human IL6	GAGGTGCCCATGCTACATTG	ATGCAATAACCACCCCTGAC
Human VCAM1	CACCTGGATTCCTTTTTCCA	CGAGACCACCCCAGAATCTA
Human ICAM1	TCACACTGACTGAGGCCTTG	GGCTGGAGCTGTTGAGAAC
Human MCP1	TGGAATCCTGATCCCACTTC	CCCCAGTCACCTGCTCTTAT
Human MMP1	TGCTTGACCCTCAGAGACCT	GATGTGGAGTGCCTGATGTG
Human MMP9	CTCCACTCCTCCCTTTCCTC	AGTTCCCGGAGTGAGTTGAA
Human $p21^{CIP1}$	AGGTGAGGGGACTCCAAAGT	ACTTCCTCCTCCCCACTTGT
Murine MMP1	TTTCTCGGAGCCTGTCAACT	ATCCTGGCCACCTTCTTCTT
Murine MMP9	GTGGATAGCTCGGTGGTGTT	TGAATCAGCTGGCTTTTGTG
Murine $p21^{CIP1}$	AGGGCCCTACCGTCCTACTA	GCCTTAGCCCTCACTCTGTG
Murine VEGFA	AATGCTTTCTCCGCTCTGAA	CAGGCTGCTGTAACGATGAA
Murine VEGFR2	GTCACTGACAGAGGCGATGA	GGCGGTGGTGACAGTATCTT
Human Ets1	TCTGCAAGGTGTCTGTCTGG	TGGAGTCAACCCAGCCTATC
Murine IL6	TCCACGATTTCCCAGAGAAC	AGTTGCCTTCTTGGGACTGA
Murine MCP1	ACCCTGGGACAAGTTGACTG	GGACGCAAAAACTACCCTGA
Murine Ets1	GGTGAGGCGGTCACAACTAT	TCCAGACAGACACCTTGCAG
Murine Ets2	TGCCTGGAAAACCCAGTTAC	TCCATATGGCCTCTCCACTC
Murine HPRT	TCAGGAGAGAAAAGATGTGATTGA	CAGCCAACACTGCTGAAACA

Human **ADAM10**	CCCAGGTTTCAGTTTGCATT	AGCAACATCTGGGGACAAAC

Discussion

Previously, Moulton and coworkers demonstrated that inhibition of neovascularization of the atherosclerotic region reduced intraplaque macrophage accumulation in advanced atherosclerosis[2]. Increase of monocyte infiltration into the atherosclerotic plaque area could also have attributed to plaque growth and destabilization. Indeed, in our murine atherosclerotic VP model, Ets2 expression promoted infiltration of CD68+ macrophages in the intima. Ets2 expression was induced in the endothelium of ApoE-/- in response to a pro-atherogenic diet, and was specifically upregulated in vulnerable atherosclerotic plaques. In addition, Ets2 expression and translocation to the nucleus is induced in response to pro-atherogenic TNFα stimulation, while Ets2 levels in human carotid endarterectomy material of atherosclerotic lesions also correlated with intra-plaque TNFα levels. In atherogenesis, TNFα is a key cytokine for the recruitment and activation of inflammatory cells via upregulation of adhesion molecules and cytokine/chemokine release by ECs[3]. TNFα level is also associated with an increased risk for cardiovascular MACE[4, 5], whereas TNFα/ApoE double knockout mice develop less advanced atherosclerotic lesions[3], demonstrating the important role of TNFα in lesion progression. In the current study, TNFα induced expression and secretion of the pro-atherogenic cytokines, MCP1 and IL6, were highly dependent on Ets2. MCP1 is a known chemo-attractant in the process of monocyte recruitment during atherosclerosis development[6, 7], while the importance of IL6 in atherogenesis was demonstrated in IL6/ApoE double knockout mice that showed a significant reduction in intraplaque macrophage infiltration[8]. Promoter regions of IL6 and MCP1 both contain multiple Ets recognition sequences. Indeed, it was previously shown that Ets2 directly regulates MCP1

transcription[9]. Our findings on the regulatory function of Ets2 in MCP1/IL6 expression underline the importance of this gene in ECs in the initial and progressive immune response during atherosclerosis development. The significant increase in infiltrating intimal macrophages in the current study could be linked to the pro-inflammatory regulatory function of Ets2 in the ECs in the vasa vasorum, as it may promote monocyte adhesion and extravazation via VCAM1, IL6, and MCP1 upregulation, while promoting microvessel formation in the atherosclerotic area with deficient vascular integrity as a secondary route of entry for inflammatory cells. In support of these findings, Ets2 protein levels in human lesions correlated with MCP1, IL6 and TNFα cytokine levels, indicating that Ets2 indeed is an important regulator of the endothelial pro-inflammatory state.

Wei and colleagues showed that mutation of both Ets1 and Ets2 during murine embryonic development induced striking defects in the vasculature. Further studies identified an anti-apoptotic role for Ets2 and Ets1 in endothelial cells, with functional redundancy in regulating endothelial cell survival during embryogenesis[10]. Theoretically, induction of Ets2 overexpression by adenoviral transfection might induce overlap function of Ets1 *in vitro* and *in vivo*. To rule out non-specific effects of Ets2 overexpression by cross-activation of Ets1 target genes, we examined the expression of a panel of genes that is known to be regulated by Ets1, including MMP1, MMP9, $p21^{CIP1}$, VEGFA and VEGFR2. *In vitro*, Ets2 overexpression in HUVECs failed to raise mRNA levels of the Ets1-target genes at 2 days post transfection compared to sham virus treated cultures. Similarly, *in vivo*, overexpression of Ets2 in the carotid artery of ApoE-/- animals mice did not induce VEGFA, VEGFR2, MMP1 or MMP9 mRNA expression as compared to sham virus transfected carotid arteries, at 2 days post transfection. In

contrast, upregulation of Ets2-target genes IL6 and MCP1 mRNA levels could be observed (supplemental figure III and IV). Combined, these data indicate that at least in HUVECs and our murine VP model, Ets2 overexpression does not promote non-specific cross-activation of Ets1-regulated genes.

Supplemental figures:

Figure I: Validation of specific detection of Ets2 in the Ets2-CD31 double immunostaining protocol: (A and C) Omission of the first antibody directed against Ets2 and IgG isotype control show limited background signal from the Rhodamin-labeled secondary antibody, (B) whereas ECs cells are clearly labeled using a primary antibody directed against CD31, followed by detection using a fitc-labeled secondary antibody. (D) Last panel shows the overlay of the different channels. Cell nuclei are labeled blue using conventional DAPI staining. Autofluorescence in the elastic lamina marks the medial area.

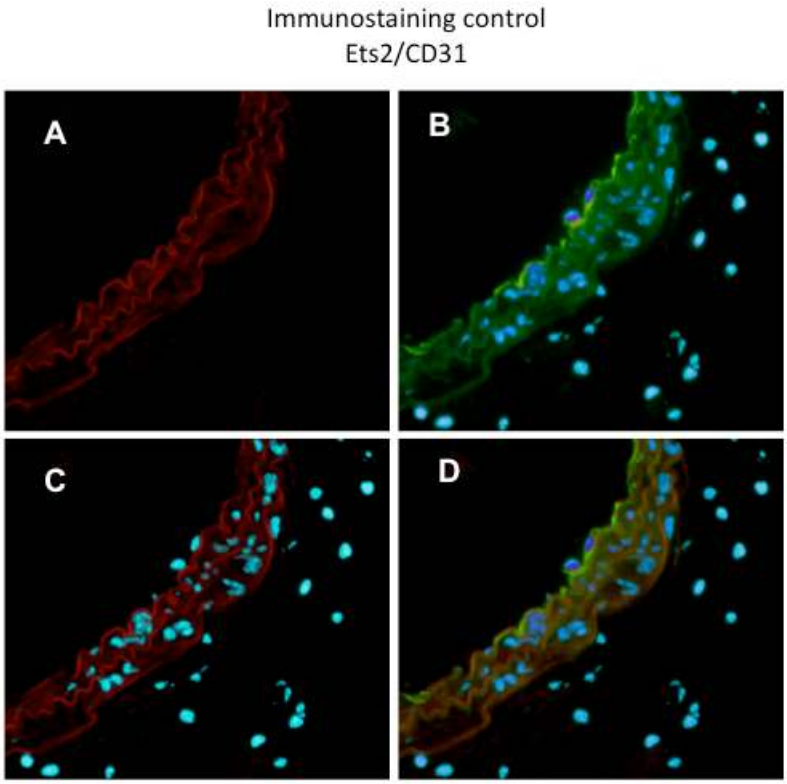

Figure II: (A) qPCR validation of human Ets2 transgene overexpression in HUVECs induced by transfection with Ets2-Ad compared to controls (ΔE1-Ad and non-transfected), at 2 days post-transfection. (*P<0,05 versus control. ‡P<0,05 versus ΔE1-Ad. N=3) (B-D) Assessment of Ets2 mRNA and protein expression in Ets2-Ad as compared to ΔE1-Ad treated animals and untreated carotid arteries after 4 days of transfection. (*P<0,05 versus control and ΔE1-Ad. N=5 for qPCR assessment; *P<0,05 versus control and ΔE1-Ad. N=10 (In two pools of 5) for westernblot analysis) (E) Immuno-histological detection of Ets2 (red fluorescent signal) in ΔE1-Ad transfected and Ets2-Ad transfected carotid arteries derived from ApoE-/- mice after 4 days of transfection. IgG isotype control show limited background signal of the Rhodamin-labeled secondary antibody. Cell nuclei are identified by DAPI.

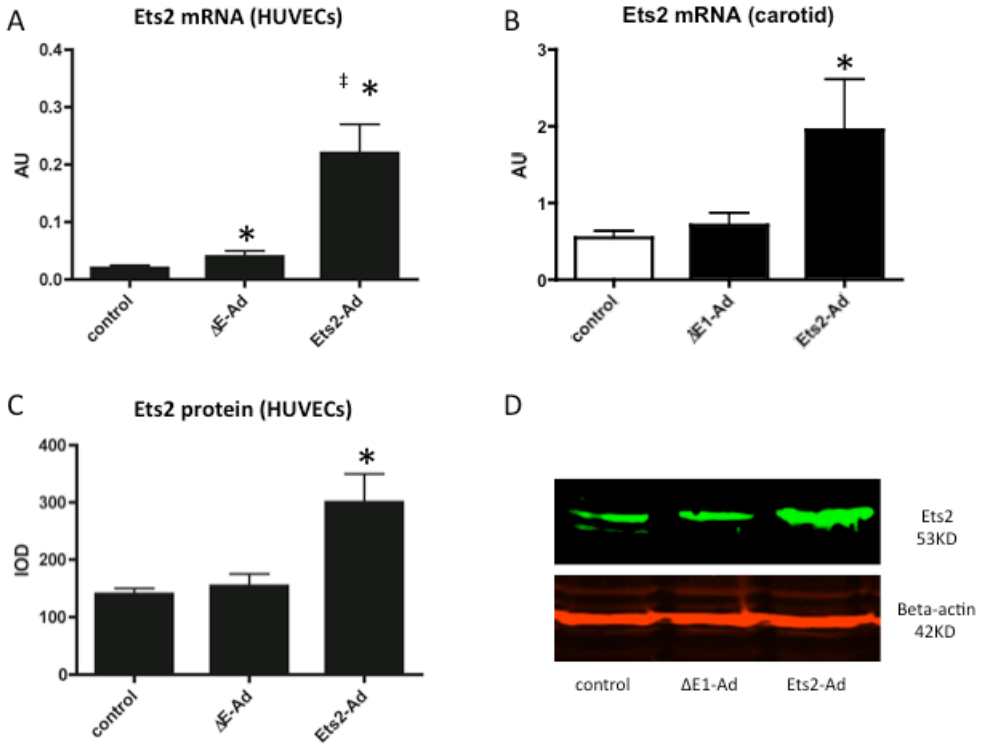

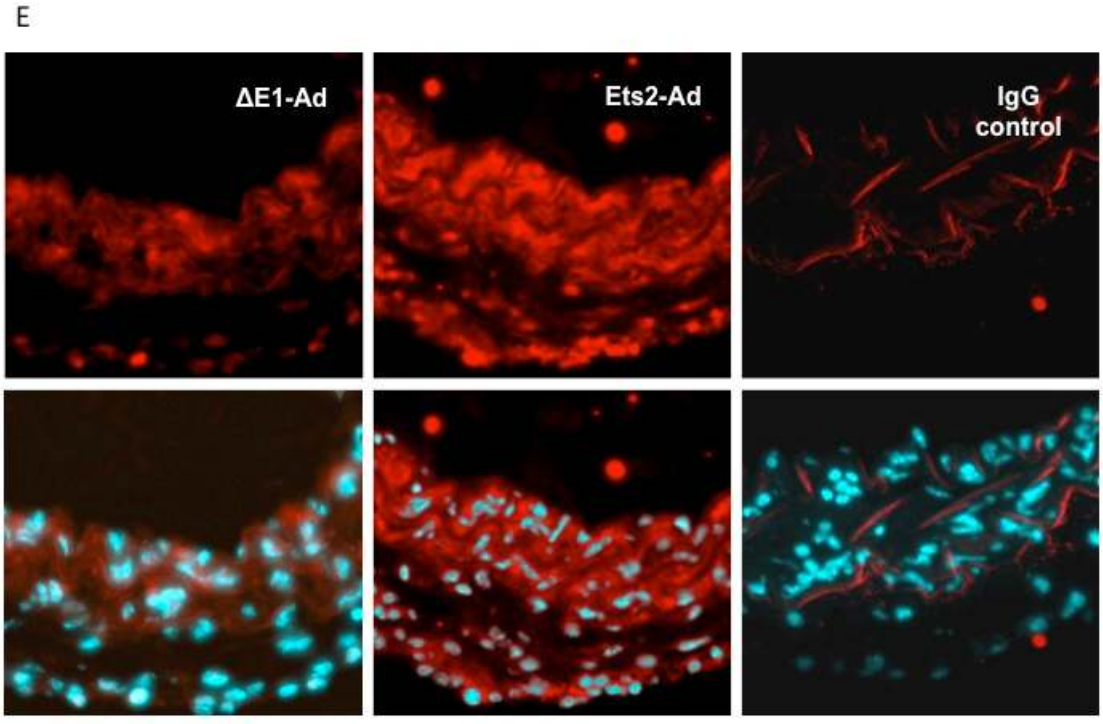

Figure III: Ets2 silencing inhibits tube-formation in ECs *in vitro*. (A) HUVECs transfected with scrambled siRNA or Ets2-targeting siRNA were cultured in a 2D matrigel to induce tube formation. Tubes were visualized by Calcein Am dye fluorescence after 18 hours of tube formation, and were assessed by fluorescence microscopy. Typical results of 5 independent experiments are shown. siRNA-mediated Ets2 silencing decreased the angiogenic capacity of HUVECs, demonstrated by a decrease in (B) number of tubes, (C) number of junctions (D) total tube length, and (E) average tube length. Ets2 remains crucial for the angiogenic response of ECs under TNFα stimulation. (N=5; *P<0,05 versus sisham or sisham +TNFα.)

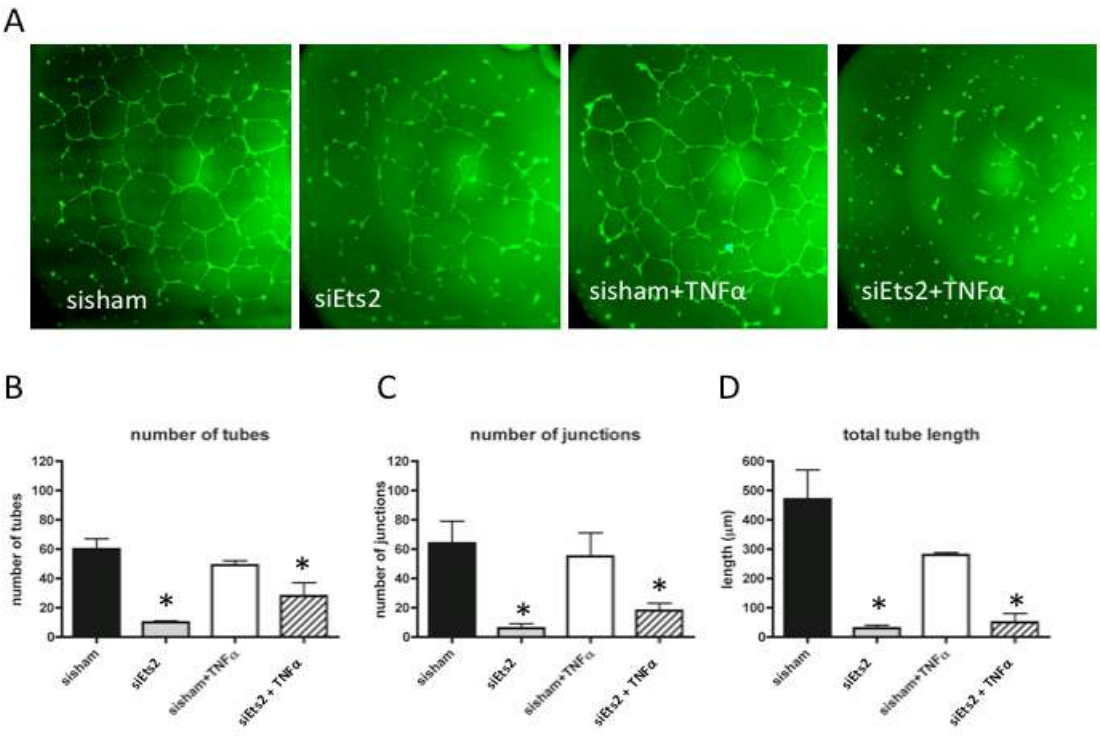

E

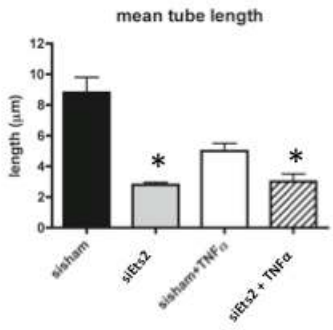

Figure IV: qPCR evaluation of possible cross-transcriptional activation of Ets1 regulated genes by adenovirus-mediated Ets2 overexpression in the carotid artery of APOE-/- mice. mRNA expression levels of Ets1 regulated genes, including VEGFA, VEGFR2, MMP1, MMP9, and $p21^{CIP1}$ were assessed in Ets2-Ad or ΔE1-Ad transfected carotid arteries. No significant effect on mRNA levels of Ets1, VEGFA, VEGFR2, $p21^{CIP1}$, MMP1, and MMP9 levels were observed 2 days after transfection, whereas mRNA levels of Ets2 responsive genes MCP1 and IL6 were upregulated in Ets2-Ad transfected carotid arteries versus sham virus transfected controls (*P<0,05 versus ΔE1-Ad. N=6).

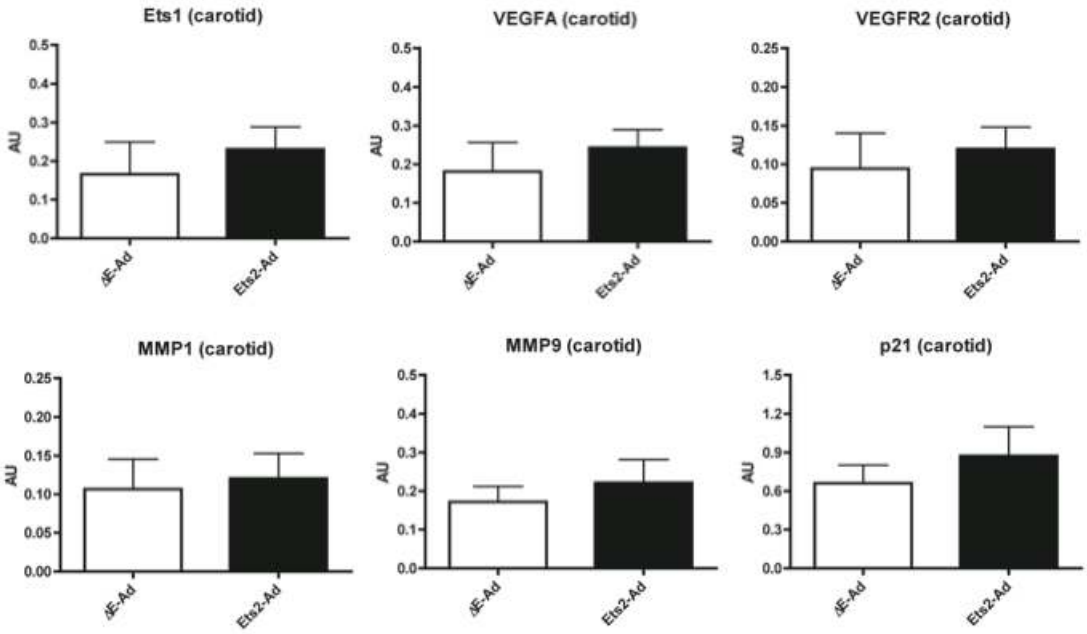

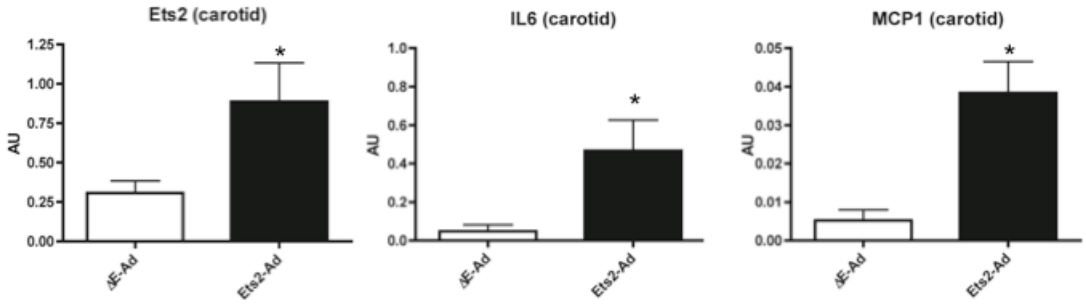

Figure V: qPCR analysis for possible cross-transcriptional activation of Ets1 regulated genes by adenovirus-mediated Ets2 overexpression in HUVECs. mRNA expression levels of by Ets1 regulated genes, including MMP1, MMP9, and $p21^{CIP1}$, were assessed in non-transfected controls, in sham virus transfected controls, and in Ets2 overexpressing ECs. Although Ets2 was significantly upregulated in Ets2-Ad transfected HUVECs, no significant effect on the mRNA levels of Ets1, $p21^{CIP1}$, MMP1, and MMP9 was observed 3 days after transfection (*P<0,05 versus ΔE1-Ad. N=3).

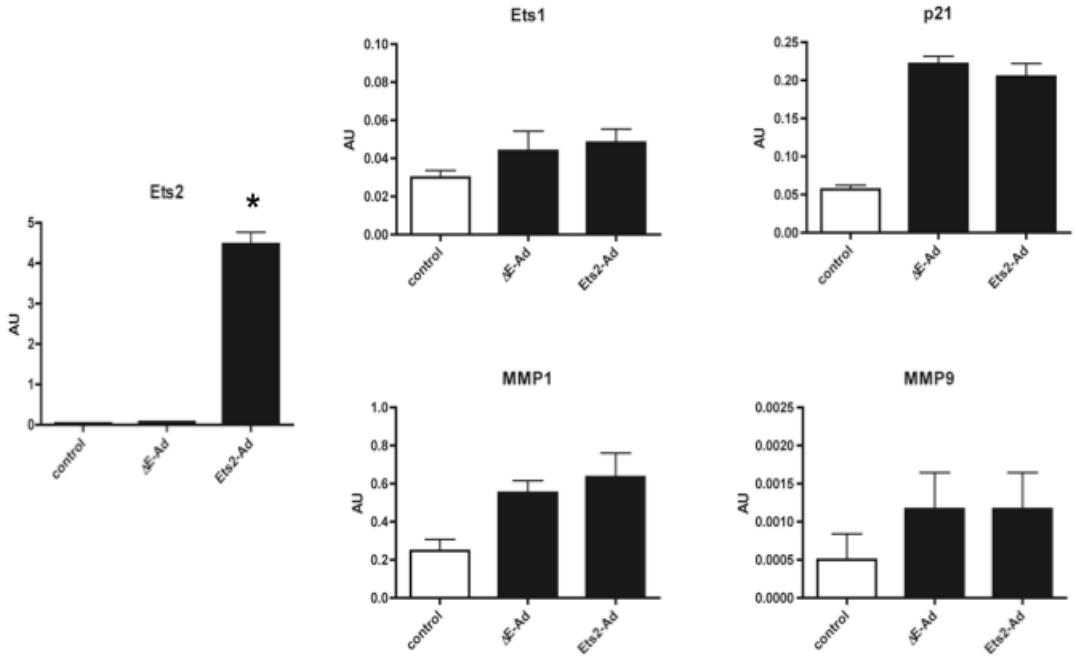

Table I: Ets2 level distribution

Quartile	1	2	3	4
Median(ng/ml)	171.6	250.1	376.1	637.6
Range (ng/ml)	187.1	67.7	154.0	764.5

Table II: Patient baseline characteristics

Risk factors	N=91 patients Median ± range
Total cholesterol (mmol/L)	4,39 ± 5,07
Total triglycerides (mmol/L)	1,30 ± 3,35
Total HDL (mmol/L)	1,04 ± 1,81
Total LDL (mmol/L)	2,54 ± 4,37
Gender (N)	Male (60) Female (31)
Systolic pressure (mm Hg)	160 ± 140
Diastolic pressure (mm Hg)	85 ± 75
Age (years)	69 ± 38
Smoking (N)	76
Diabetes (N)	24
Hypercholesterolemia (N)	66

References:

1. Cheng C, Noordeloos AM, Jeney V, Soares MP, Moll F, Pasterkamp G, Serruys PW, Duckers HJ. Heme oxygenase 1 determines atherosclerotic lesion progression into a vulnerable plaque. *Circulation.* 2009;119:3017-3027.

2. Moulton KS, Vakili K, Zurakowski D, Soliman M, Butterfield C, Sylvin E, Lo KM, Gillies S, Javaherian K, Folkman J. Inhibition of plaque neovascularization reduces macrophage accumulation and progression of advanced atherosclerosis. *Proc Natl Acad Sci U S A.* 2003;100:4736-4741.

3. Branen L, Hovgaard L, Nitulescu M, Bengtsson E, Nilsson J, Jovinge S. Inhibition of tumor necrosis factor-alpha reduces atherosclerosis in apolipoprotein E knockout mice. *Arterioscler Thromb Vasc Biol.* 2004;24:2137-2142.

4. Ridker PM, Cushman M, Stampfer MJ, Tracy RP, Hennekens CH. Inflammation, aspirin, and the risk of cardiovascular disease in apparently healthy men. *N Engl J Med.* 1997;336:973-979.

5. Ridker PM, Glynn RJ, Hennekens CH. C-reactive protein adds to the predictive value of total and HDL cholesterol in determining risk of first myocardial infarction. *Circulation.* 1998;97:2007-2011.

6. Aiello RJ, Bourassa PA, Lindsey S, Weng W, Natoli E, Rollins BJ, Milos PM. Monocyte chemoattractant protein-1 accelerates atherosclerosis in apolipoprotein E-deficient mice. *Arterioscler Thromb Vasc Biol.* 1999;19:1518-1525.

7. Kowala MC, Recce R, Beyer S, Gu C, Valentine M. Characterization of atherosclerosis in LDL receptor knockout mice: macrophage accumulation correlates with rapid and sustained expression of aortic MCP-1/JE. *Atherosclerosis.* 2000;149:323-330.

8. Schieffer B, Selle T, Hilfiker A, Hilfiker-Kleiner D, Grote K, Tietge UJ, Trautwein C, Luchtefeld M, Schmittkamp C, Heeneman S, Daemen MJ, Drexler H. Impact of interleukin-6 on plaque development and morphology in experimental atherosclerosis. *Circulation.* 2004;110:3493-3500.

9. Zhan Y, Brown C, Maynard E, Anshelevich A, Ni W, Ho IC, Oettgen P. Ets-1 is a critical regulator of Ang II-mediated vascular inflammation and remodeling. *J Clin Invest.* 2005;115:2508-2516.

10. Wei G, Srinivasan R, Cantemir-Stone CZ, Sharma SM, Santhanam R, Weinstein M, Muthusamy N, Man AK, Oshima RG, Leone G, Ostrowski MC. Ets1 and Ets2 are required for endothelial cell survival during embryonic angiogenesis. *Blood.* 2009;114:1123-1130.